



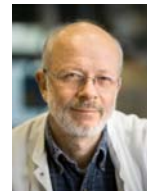
# PET

(and PET/CT, PET/MR, and SPECT/CT)

Medical Imaging Systems  
DTU, November 2018

Søren Holm

Senior Physicist, ph.d.  
PET- and Cyclotron Unit, Rigshospitalet



1



## Rigshospitalet, Copenhagen

PET

Entrance 39



©2018

Photo: Flying Professor Andreas Kjær

2

## Thanks to:

GE Medical Systems  
CPS Innovation (Bernard Bendriem)  
Siemens Medical Solutions  
Philips Medico  
Impact ([www.impactscan.org](http://www.impactscan.org))  
UC Davis, Simon Cherry



## Overview (0):

- Different kinds of tomography – PET in particular
  - Reconstruction from projections, FBP vs. iterative methods
  - Positron imaging history
  - Raw data structure - sinograms - types of acquisition and presentation
  - 2D/3D, advanced data structure – Michelogram
- 
- Resolution and noise
  - Scanner physics 1 – PET detectors
  - Scanner physics 2 – good, bad, and noise equivalent counts (NEC)
  - Attenuation and scatter correction of PET-data
  - Hybrid systems – PET/CT- PET/MR - SPECT/CT... Future ideas

**(T)CT**  
Computer(ized)

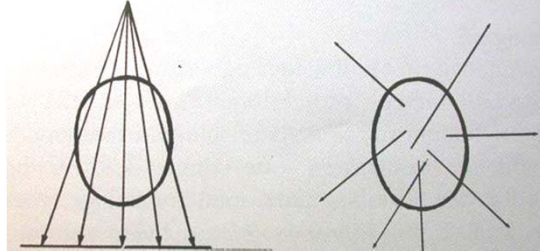
**ECT**  
SPECT  
PET

from:



**TRANSMISSION**

**EMISSION**

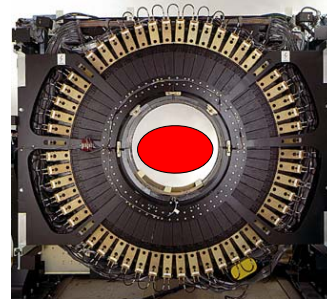
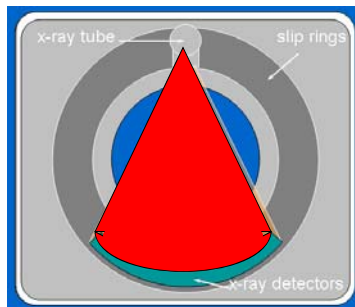


**attenuation of photons**  
**structure / anatomy**

**distribution of tracer**  
**function / physiology**

**CT**

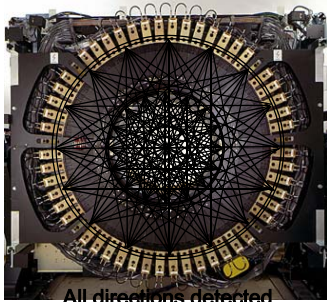
**PET**



**attenuation of photons**  
**structure / anatomy**

**distribution of tracer**  
**function / physiology**

PET is stationary – SPECT rotates

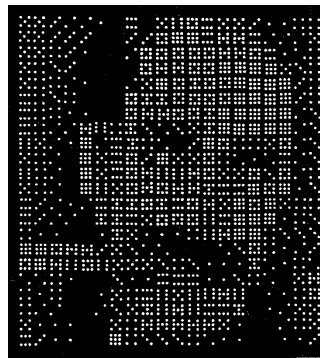
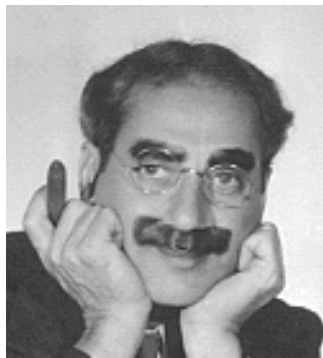


All directions detected simultaneously



Radiology

Nuclear Medicine



Ken Krowlton, Domino Portraits, 1982

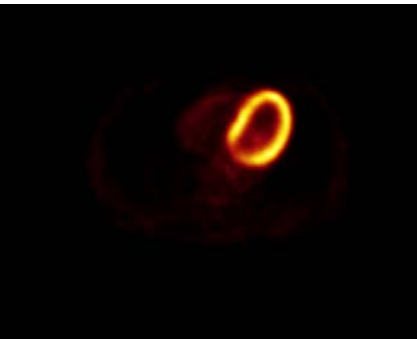
#dots recorded determine what details can be seen in image

And for those ignorants of classic entertainment : this is Groucho Marx

*"I never forget a face, but in your case I'll be glad to make an exception."*

RH 


CT                      PET

attenuation of photons  
structure / anatomy

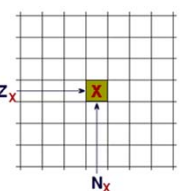
distribution of tracer  
function / physiology

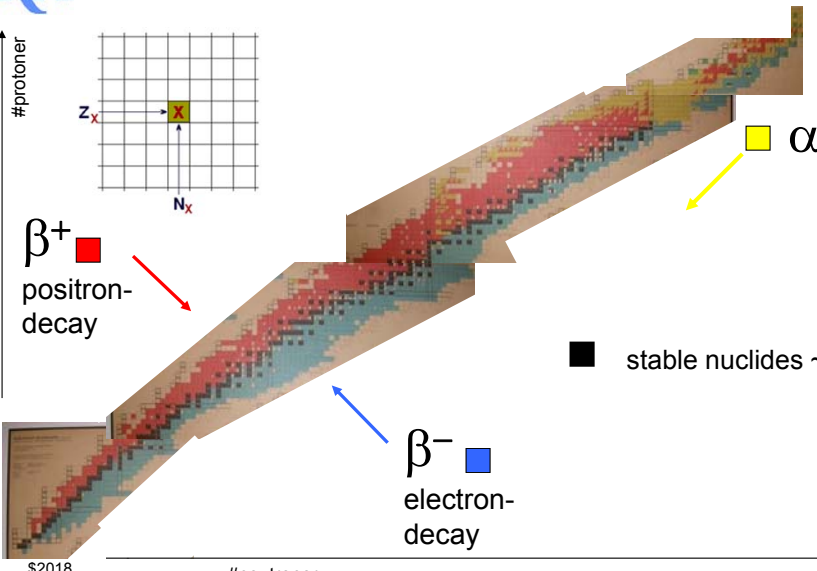
\$2018 9

RH 


The nuclear chart (N,Z) – decay types

#protoner





$\beta^+$  ■ positron-decay

$\beta^-$  ■ electron-decay

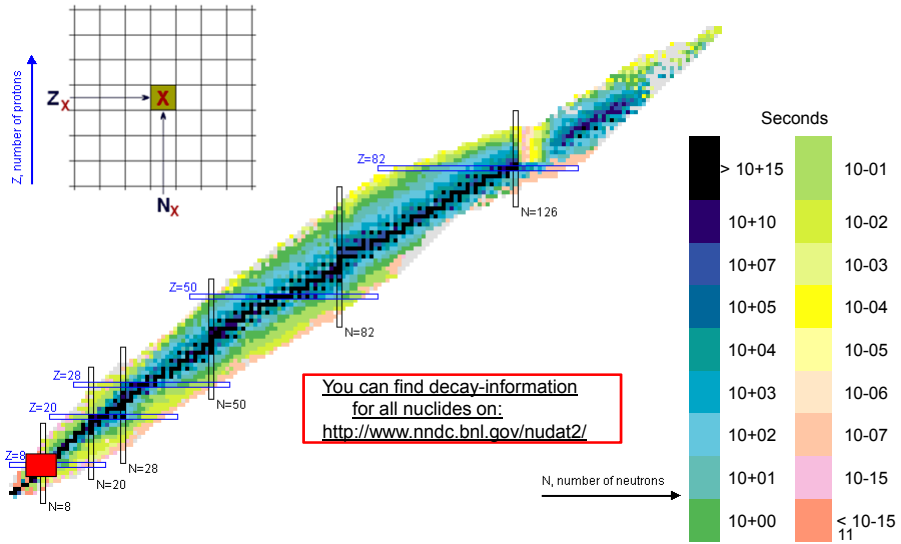
$\alpha$  ■

■ stable nuclides ~257

\$2018 10



# The nuclear chart (N,Z) – half lives



# ...magnified

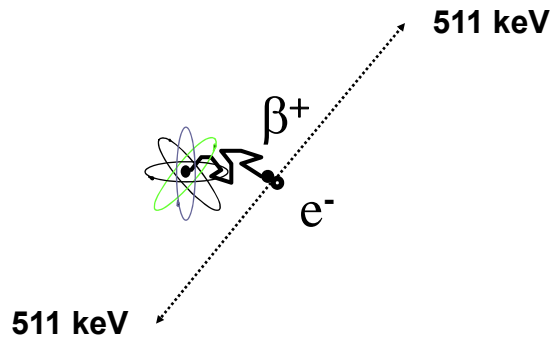


		Ne 16	Ne 17 109 ms $\beta^+$ 8.0, 13.5... $\beta\beta$ 4.59, 3.77, 5.12...	Ne 18 1.67 s $\beta^+$ 3.4... $\gamma$ 1042...	Ne 19 17.22 s $\beta^+$ 2.2... $\gamma$ (1357...)	Ne 20 90.51
		F 15	F 16	F 17 64.8 s $\beta^+$ 1.7 no $\gamma$	F 18 109.7 m $\beta^+$ 0.6 no $\gamma$	F 19 100
O 12	O 13 8.9 ms $\beta^+$ 16.7... $\beta\beta$ 1.44, 6.44, 0.93	O 14 70.59 s $\beta^+$ 1.8, 4.1... $\gamma$ 2313...	O 15 2.03 m $\beta^+$ 1.7 no $\gamma$	O 16 99,762 $\alpha$ 0.000178	O 17 0.038 $\alpha_{n,p}$ 0.235	O 18 0.200 $\alpha$ 0.00016
	N 12 11.0 ms $\beta^+$ 16.4... $\gamma$ 4439... $\beta\alpha$ 0.2...	N 13 9.96 m $\beta^+$ 1.2 no $\gamma$	N 14 99.63 $\alpha$ 0.075 $\alpha_{n,p}$ 1.81	N 15 0.37 $\alpha$ 0.000024	N 16 5,3 $\mu$ s 7,13 s $\beta^+$ 4.3... 16.4... $\beta\beta$ 0.029... $\beta\alpha$ 1.3	N 17 4.17 s $\beta^+$ 3.2, 8.7... $\beta\beta$ 1.17, 0.36... $\gamma$ 871, 2164
C 10 19,3 s 1.8... 18, 1022	C 11 20,38 m $\beta^+$ 1.0 no $\gamma$	C 12 98,90 $\alpha$ 0.0034	C 13 1,10 $\alpha$ 0,0009	C 14 5730 a $\beta^-$ 0.2 no $\gamma$	C 15 2,45 s $\beta^-$ 4,5, 9,8... $\gamma$ 5298	C 16 0,747 s $\beta^-$ 0,79, 1,72

\$2018

12

# PET *is really* ART: Annihilation Radiation Tomography



1955



$$E = mc^2$$

1905

Result: Two photons on an **almost** straight line that **nearly** contains the point of decay

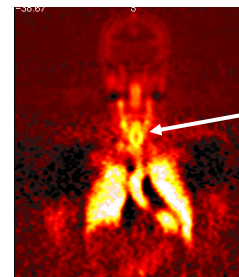
\$2018

13

# Positron Emission Tomography (?) or ART

We never detect the positrons directly, only the annihilation photons

Annihilation  
Radiation  
Tomography

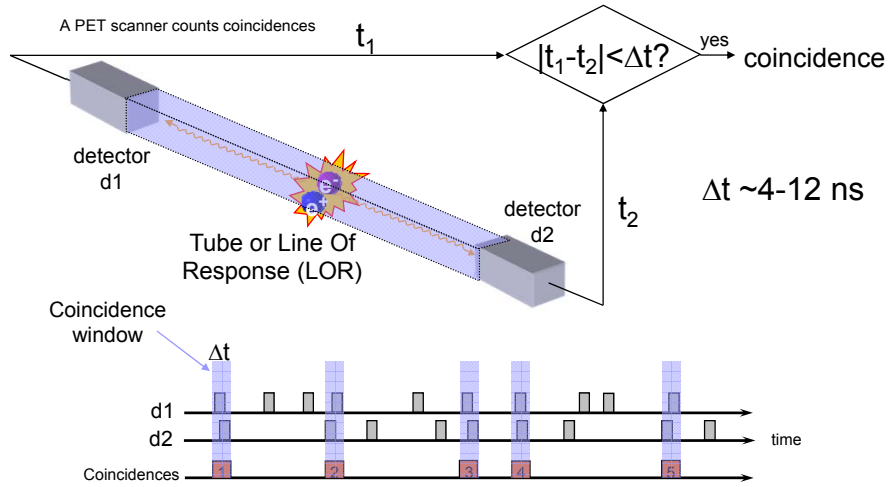


Inhalation of radioactive  $\beta^+$  gas

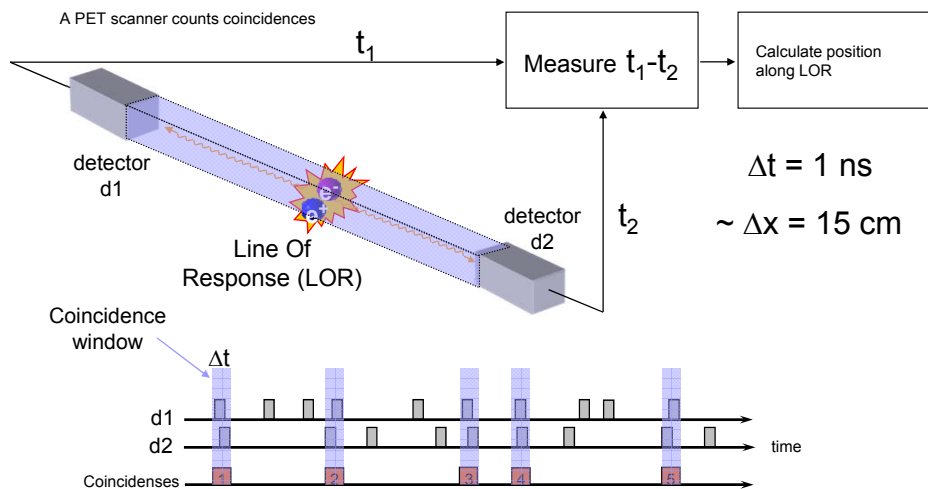
\$2018

14

# PET radiation detection

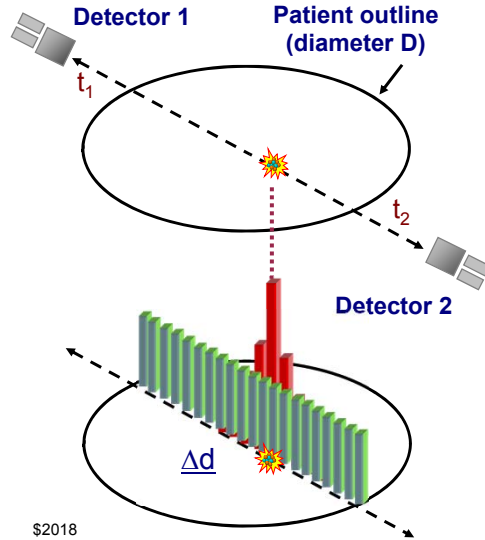


# PET detection, Time-of-Flight



# Time of Flight (TOF) PET

– more than just a coincidence...



- tried and abandoned in ancient PET times (~1985)
- idea commercially relaunched in 2006 by Philips

$\delta t$ (ps)	$\Delta d$ (cm)	SNR
100	1.5	5.2
300	4.5	3.0
500	7.5	2.3
600	9.0	2.1

- More information available for image formation
- better image quality, or shorter scanning time, or less injected activity

\$2018

17

# Positron Emitting Isotopes

Isotope	Half-Life	Production
Carbon-11	20.5 min	$^{14}\text{N}(p,\alpha)^{11}\text{C}$
Nitrogen-13	10.0 min	$^{16}\text{O}(p,\alpha)^{13}\text{N}$
Oxygen-15	2.1 min	$^{14}\text{N}(d,n)^{15}\text{O}$
<b>Fluorine-18</b>	<b>110 min</b>	$^{18}\text{O}(p,n)^{18}\text{F}$ (F <sup>-</sup> ), $^{20}\text{Ne}(d,\alpha)^{18}\text{F}$ (F <sub>2</sub> )
Gallium-68	68 min	Daughter of Ge-68 (271days)
Rubidium-82	1.3 min	Daughter of Sr-82 (25days)

- Small elements (C,N,O,F) allow “real” biochemistry
- Short half-lives make tracer production an integral part of PET

\$2018

18

# Cyclotrons

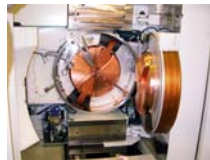


Scanditronix 32 MeV

\$2018

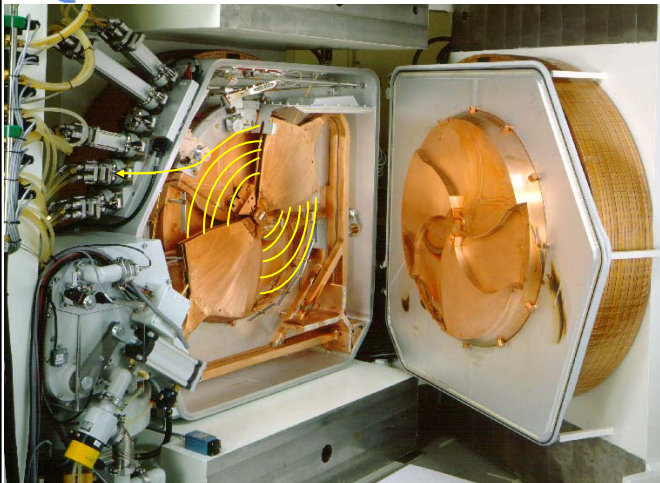


GE Minitrace 11 MeV



19

# (small) Cyclotron



**Ion Source**

Production of  $H^-$

**RF + magnetic field**

Ion acceleration

**Carbon foil**

Electron stripping

$H^- \Rightarrow H^+$  (protons!)

protons do irradiate a

**Target**

\$2018

20

## Nuclear Reactions

$^{18}\text{O} (p,n) ^{18}\text{F}$   
 $^{14}\text{N} (d,n) ^{15}\text{O}$   
 $^{14}\text{N} (p,\alpha) ^{11}\text{C}$   
 $^{16}\text{O} (p,\alpha) ^{13}\text{N}$

			$^{17}\text{F}$ 64.49s $\beta^+$	$^{18}\text{F}$ 109.77m 96.9% $\beta^+$	$^{19}\text{F}$ 20.3 ms
		$^{15}\text{O}$ 122.24s 99.9% $\beta^+$	$^{16}\text{O}$ 99.762	$^{17}\text{O}$ 0.038	$^{18}\text{O}$ 0.200
	$^{13}\text{N}$ 9.96 m $\beta^+$	$^{14}\text{N}$ 99.64	$^{15}\text{N}$ 0.36		
$^{11}\text{C}$ 20.3 m 99.8% $\beta^+$	$^{12}\text{C}$ 98.89	$^{13}\text{C}$ 1.11	$^{14}\text{C}$ 5736 a		

\$2018

21



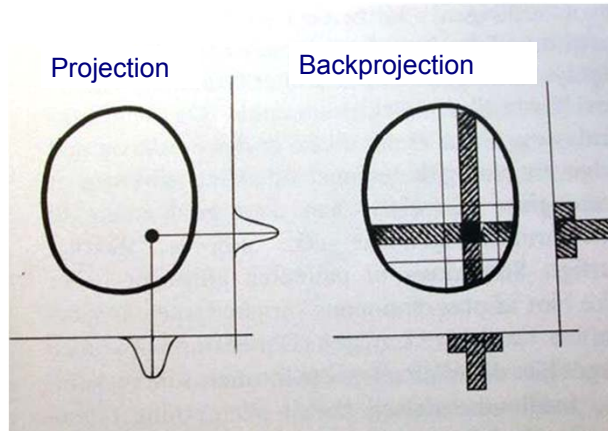
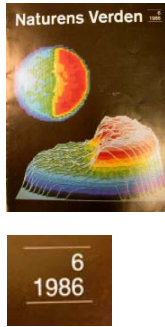
## Overview (1):

- Different kinds of tomography – PET in particular
  - Reconstruction from projections, FBP vs. iterative methods
  - Positron imaging history
  - Raw data structure - sinograms - types of acquisition and presentation
  - 2D/3D, advanced data structure – Michelogram
- 
- Resolution and noise
  - Scanner physics 1 – PET detectors
  - Scanner physics 2 – good, bad, and noise equivalent counts (NEC)
  - Attenuation and scatter correction of PET-data
  - Hybrid systems – PET/CT- PET/MR - SPECT/CT... Future ideas

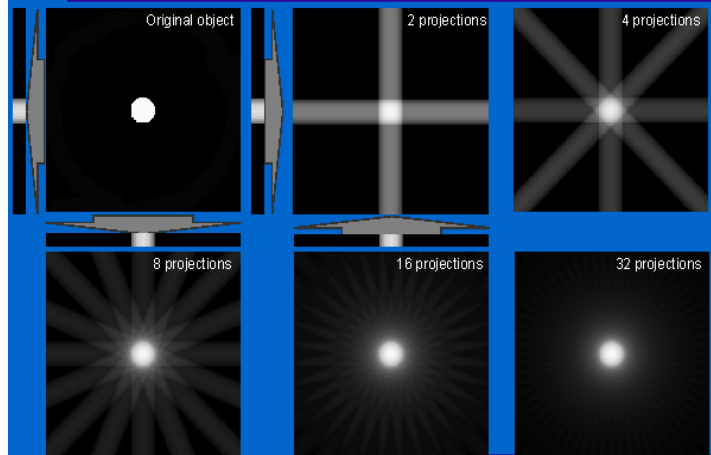
\$2018

22

# Principle of image formation!

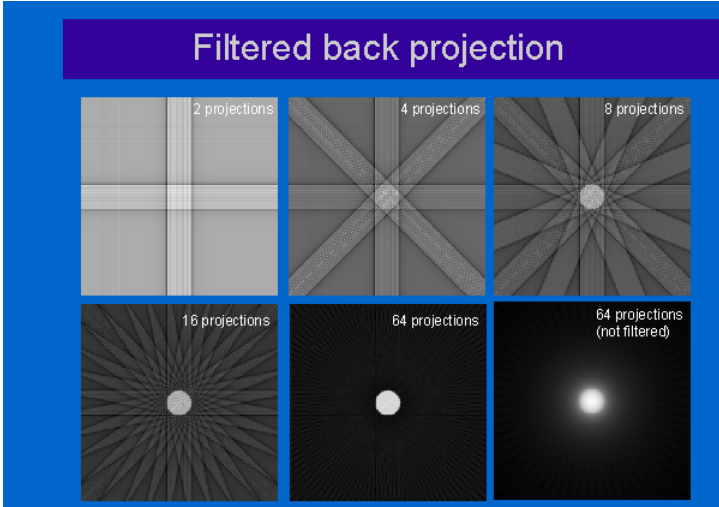


# Back projection



RH 

## Filtered back projection



2 projections      4 projections      8 projections

16 projections      64 projections      64 projections (not filtered)

\$2018 25

RH 

## Example of FBP

Filtered Back Projection of Xray-data (CT)



Institut für Medizinische Physik  
Universität Erlangen-Nürnberg

\$2018 26

**RH**

**Filtered back projection**

original

Profile  
Filtered profile

back projected image

filtered back projected image

\$2018

27

**RH**

**Iteration principle**

image space

image estimate

old

new

UPDATE

image space error

forward projection

model !!!

projection space

estimated projections

measured projections

COMPARE

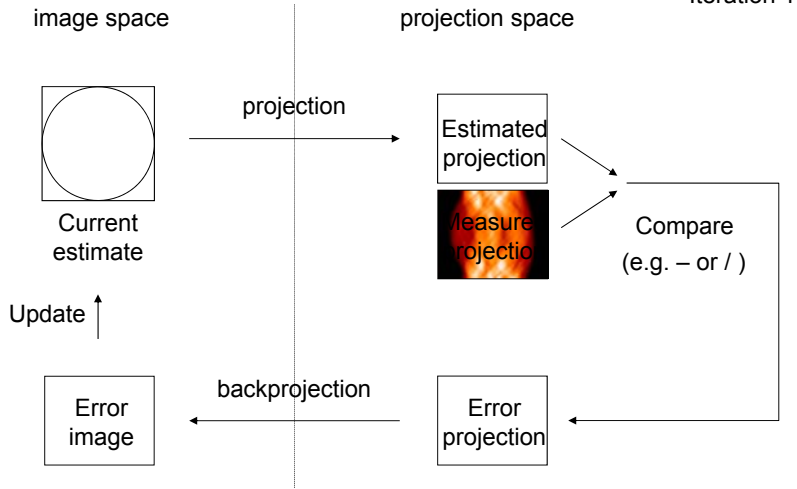
projection space error

backprojection

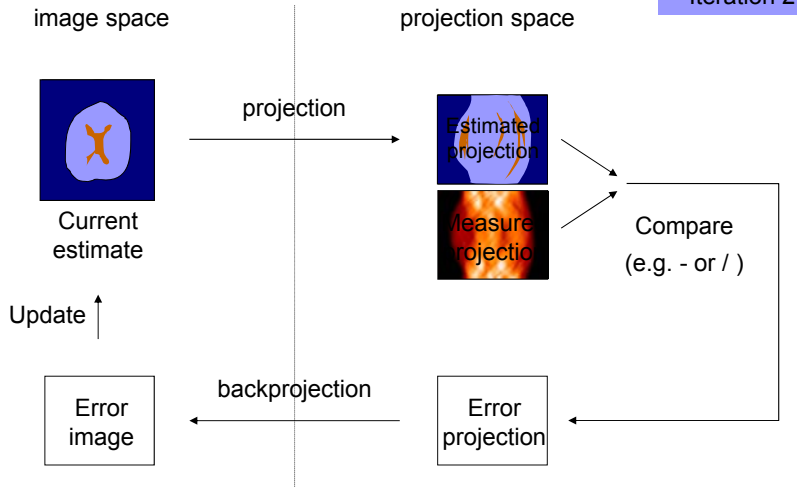
\$2018

28

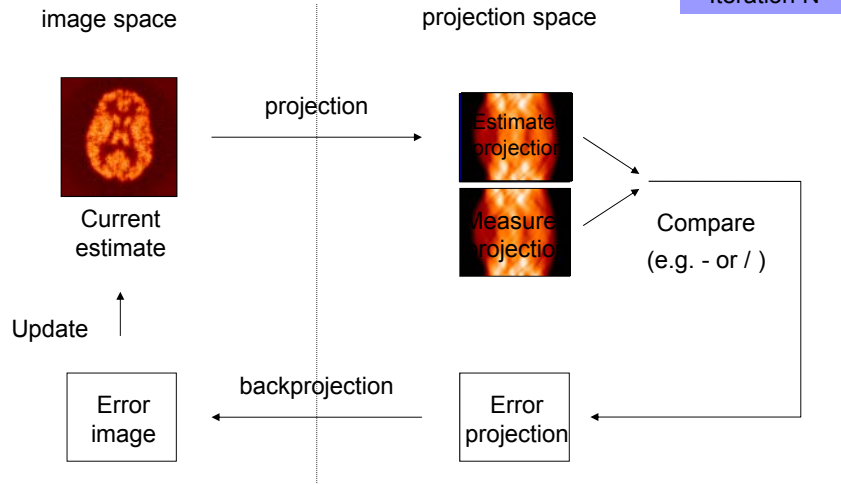
## Iterative methods



## Iterative methods

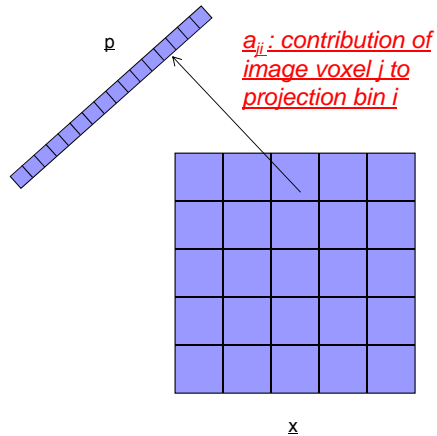


## Iterative methods

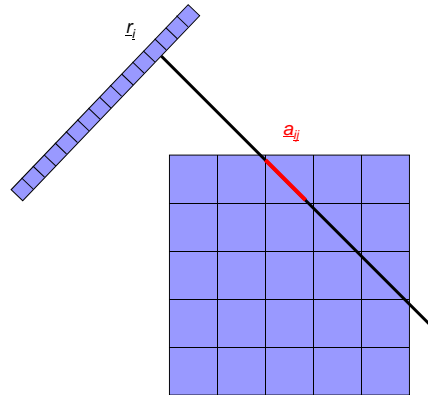


## Iterative Algorithms

- For example, ML-EM, OS-EM,
- Discretize the image into pixels
- Solve matrix equation  $\mathbf{Ax}=\mathbf{p}$
- $x$  = unknowns (pixel values)
- $p$  = projection data
- $A$  = imaging system matrix



# Line-Length Weighting



Projection ( $A$ ):

$$r_j = \sum_{j=1}^M a_{ji} x_j$$

Backprojection ( $A^T$ ):

$$x_{j,back} = \sum_{i=1}^N a_{ij} r_i$$

33

# Iterative Recon versus FBP

## FBP Methods

## Iterative Methods

**Implementation:**

Simple

Complex

**Reconstruction speed:**

Very fast

Slow with ML-EM, fast with OSEM

**Imbedded corrections:**

None

anything you can model

**Low-count image:**

Noisy

Less noise

**Reconstruction artifacts:**

Streak/spill artifacts

None, regular activity distribution



FBP reconstructed image

\$2018

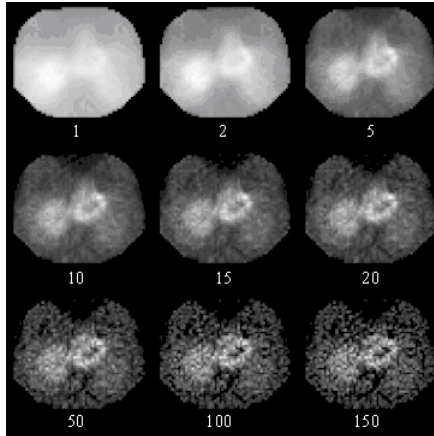


OSEM reconstructed image

34

# Image at different iteration numbers

Smooth  
Low resolution



Noisy  
High resolution

# Time to breathe...



[Reykjavik, 25. August 2011\$]

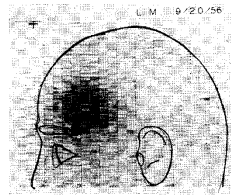
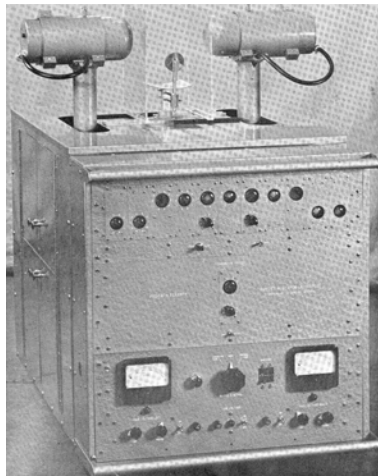


## Overview (2):



- Different kinds of tomography – PET in particular
  - Reconstruction from projections, FBP vs. iterative methods
  - Positron imaging history
  - Raw data structure - sinograms - types of acquisition and presentation
  - 2D/3D, advanced data structure – Michelogram
- 
- Resolution and noise
  - Scanner physics 1 – PET detectors
  - Scanner physics 2 – good, bad, and noise equivalent counts (NEC)
  - Attenuation and scatter correction of PET-data
  - Hybrid systems – PET/CT- PET/MR - SPECT/CT... Future ideas

## Positron scanner (*not PET*) (Brain tumor scanner at MGH 1955- )



Positrocephalogram (PCG)  
of patient with meningioma



# COINCIDENCE SCANNING WITH POSITRON-EMITTING ARSENIC OR COPPER IN THE DIAGNOSIS OF FOCAL INTRACRANIAL DISEASE

(IAEA meeting 1959)



By  
William H. SWEET, John MEALEY, Jr.,  
Gordon L. BROWNELL and Saul ARONOW  
Departments of Surgery and Medicine, Harvard Medical School, and the  
Neurosurgical Service and Physics Research Laboratory of  
Massachusetts General Hospital, Boston, Massachusetts, U. S. A.

## MEDICAL RADIOISOTOPE SCANNING

Proceedings  
of a seminar jointly organized by  
The International Atomic Energy Agency and the World Health Organization  
Vienna, 25 — 27 February, 1959

### Abstract

This is a report on coincidence counting in man of the paired annihilation gamma rays from positron-emitting copper or arsenic. We discuss the relevant biological behavior of inorganic arsenate and arsenite, of copper versenate, and the results of using these substances during automatic scanning to localize intracranial masses.

Radioassay of biopsies of the principal normal cephalic tissues, of various types of neoplasms, of hematomas, abscesses and zones of demyelination were carried out. With arsenic the ratios of concentrations of tumor to normal brain were up to 30 for meningiomas. The remaining main tumor types, in order of decreasing concentrations of isotope, were acoustic neuroma, glioblastoma, metastatic malignancy and astrocytoma. The high tumor uptake with arsenic persists long enough so that repeat scans one day after injection are valuable. The muscle : brain ratio of concentrations of circa 3 is high enough to interfere with the accuracy of diagnosis in lesions beneath the lower temporal and especially the upper nuchal masses of muscle. Hematomas, abscesses and zones of demyelination also have high enough ratios to permit localization in the majority of patients. The results on biopsies containing copper versenate showed similar ratios insofar as ascertainable from fewer samples. The meningiomas are a probable exception, yielding lower ratios with the copper.

On the basis of radioassay both of urinary excretion and of the full range of tissues obtainable at autopsy we compute the local whole-body radiation with As<sup>74</sup> to be about 3.2 rads after the usual scanning dose of 2.3 mC/70 kg. The kidney receives about 12.7 and the liver 9.7 rads. The corresponding figures for Cu<sup>64</sup> are 0.325 rads to the whole body, but with a dose to the liver of 3.2 rads because this organ takes up about half of the administered versenate.

The automatic scan includes in 2 simultaneously evolving side views a coincidence count or positronophotonogram (PCG) and a plot of the asymmetry of the total gamma radiation, or asymmetrogamma (AGC). A sagittal PCG is also taken. The lateral scan requires 40 minutes, the sagittal 20 minutes.

Of the more than 3000 scans carried out we report here only the 285 performed in the last 3 1/2 years on a special group of 334 patients, who nearly all proved to have

PCG:  
A "routine" examination!



# Anger camera (Rev.Sci.Instr. 1957)

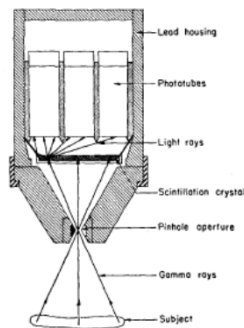


FIG. 1. Sectional drawing of scintillation camera.

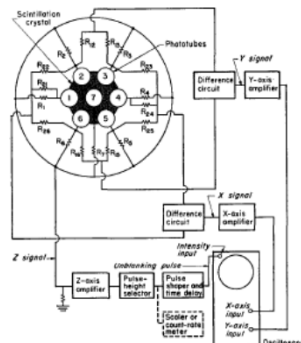
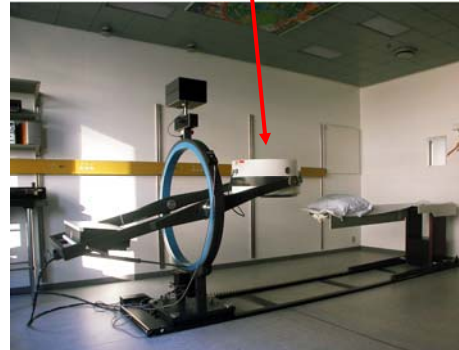
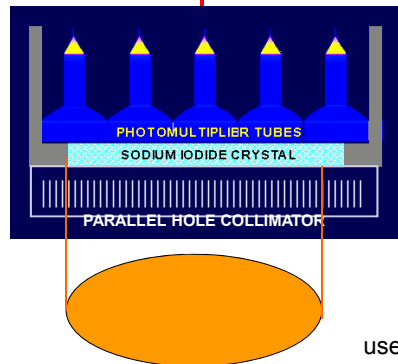


FIG. 2. Block diagram of electronic circuit.

## Gamma camera principle

position sensitive photon-detector



used for planar imaging or tomography (SPECT)

\$2018

41

### NEW POSITRON TECHNIQUE

The Anger positron camera has proven to be of considerable value in high-sensitivity scanning.<sup>3</sup> This camera, shown in Figure 12, consists of a conventional Anger camera coupled



**NUCLEAR-CHICAGO**

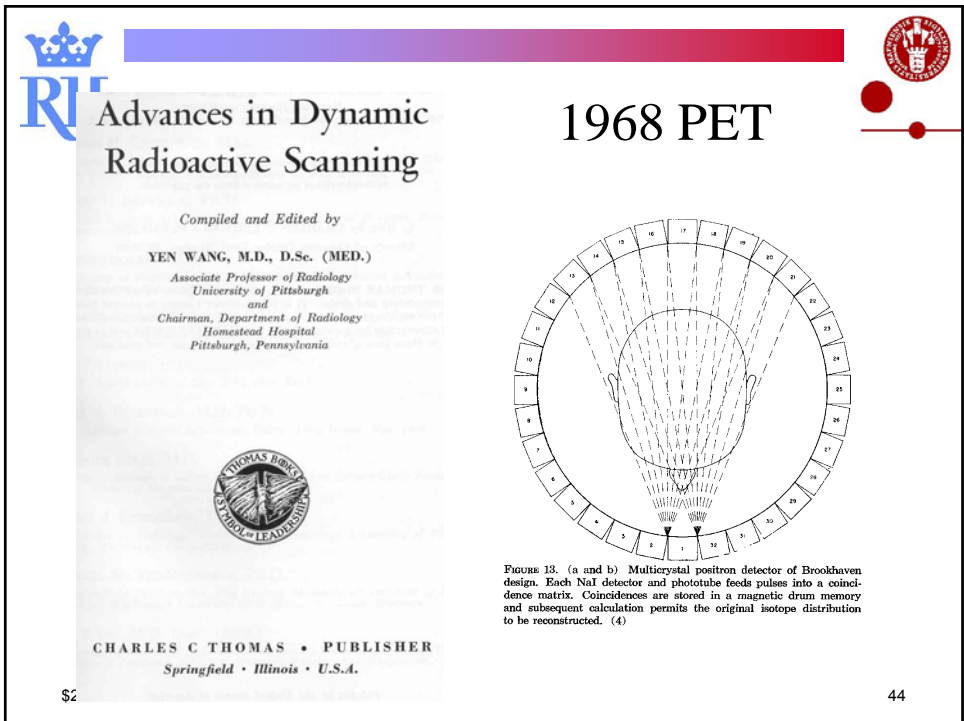
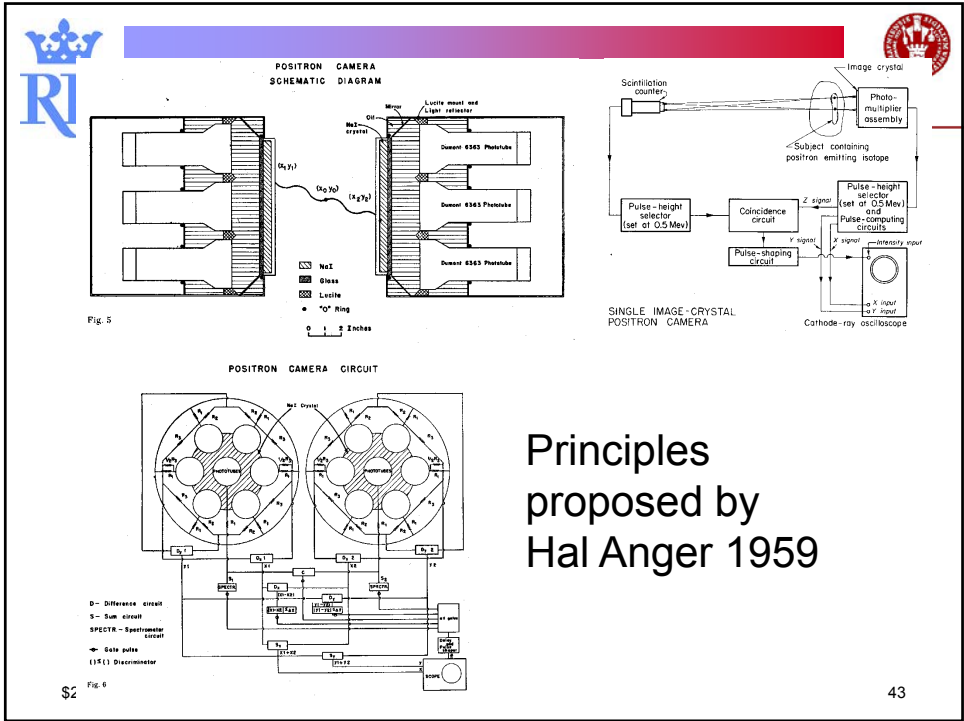
FIGURE 12. Anger positron camera. The crystal matrix is used to select and position pulses from the Anger scintillation camera. (3)

with a second matrix of sodium-iodide detectors. Only pulses in the scintillation camera which are coincident with pulses in the detector matrix are recorded. The position of the pulses are adjusted according to the location of the detector in the second matrix. By a simple control, it is possible to focus on various planes within the object. Because of the very-wide-

Gamma camera for positron imaging:

NOT a recent invention

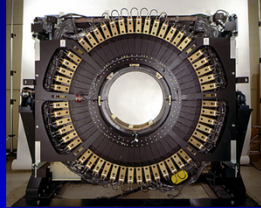
42



# PET 1966 -



Positome I 1966  
32 detectors



Advance 1993  
12096 detectors



Therascan 1982  
256 detectors

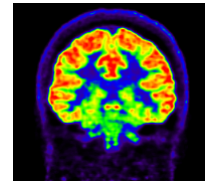
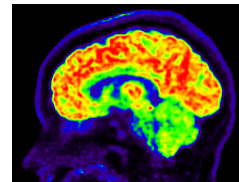
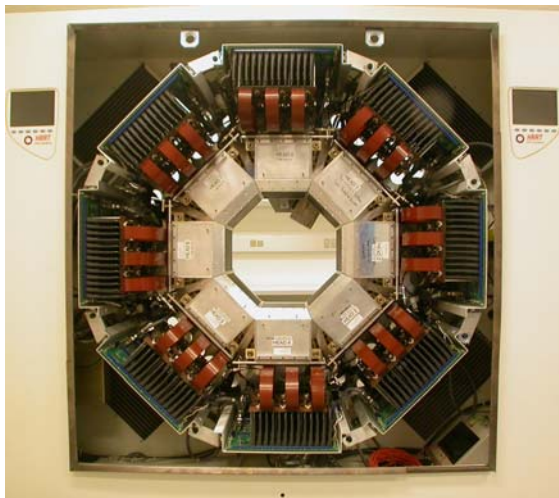


HRRT 2002  
119,808 detectors

\$2018

\$2002

# Special Brain scanner (HRRT)



119,808  
Detector  
elements

\$2018

46

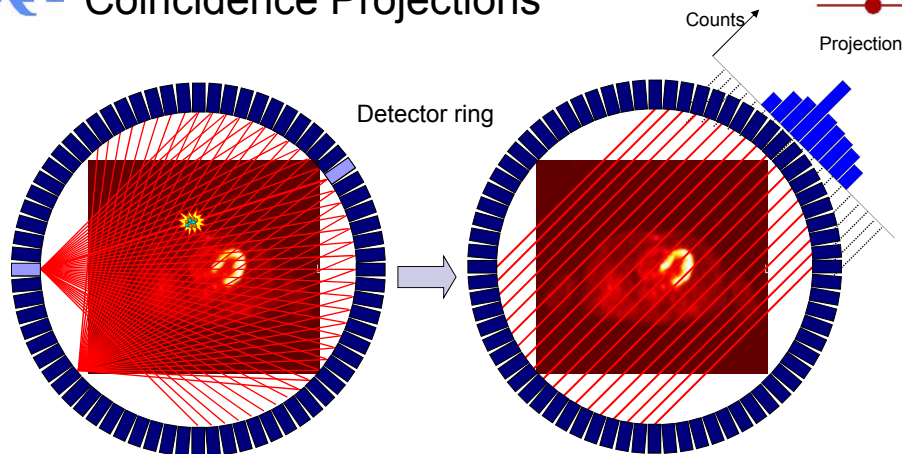


## Overview (3):



- Different kinds of tomography – PET in particular
  - Reconstruction from projections, FBP vs. iterative methods
  - Positron imaging history
  - Raw data structure - sinograms - types of acquisition and presentation
  - 2D/3D, advanced data structure – Michelogram
- 
- Resolution and noise
  - Scanner physics 1 – PET detectors
  - Scanner physics 2 – good, bad, and noise equivalent counts (NEC)
  - Attenuation and scatter correction of PET-data
  - Hybrid systems – PET/CT- PET/MR - SPECT/CT... Future ideas

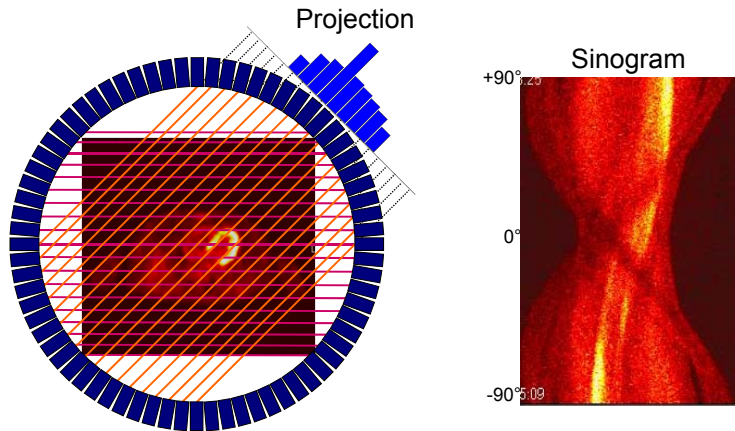
## Coincidence Projections



Coincidence events determine sampling paths (**Lines Of Response**)

Parallel Lines Of Response are sorted into a row of count numbers (**Projection**), representing the number of 511 keV photon pairs detected.

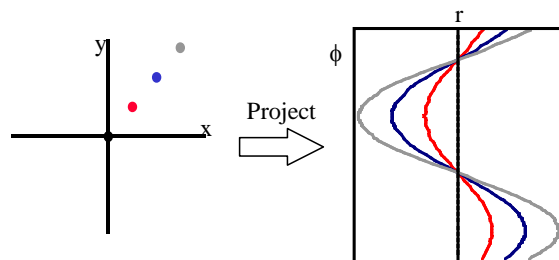
## Data-Sorting Sinogram



Each **projection** is entered as a row into a **sinogram**. A sinogram is an array which stores the number of coincidence events for each detector **position** and each **angle**.

## Sinogram

Real Space

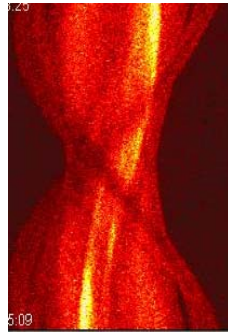


Radon transform

Point in center: straight line

Off-center: sine curve, amplitude proportional to radius

# Image Reconstruction



Sinogram

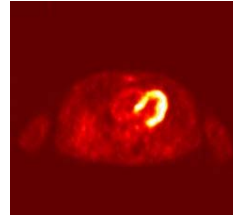
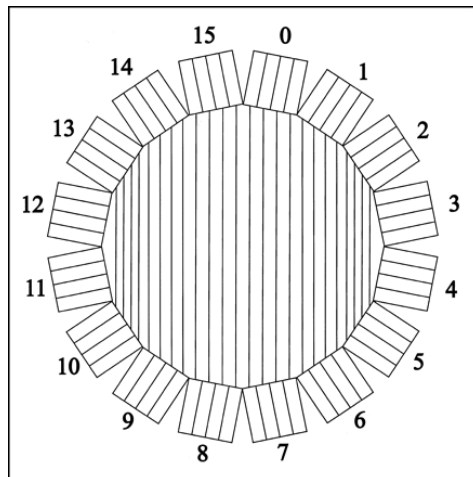


Image slice

# Geometric correction

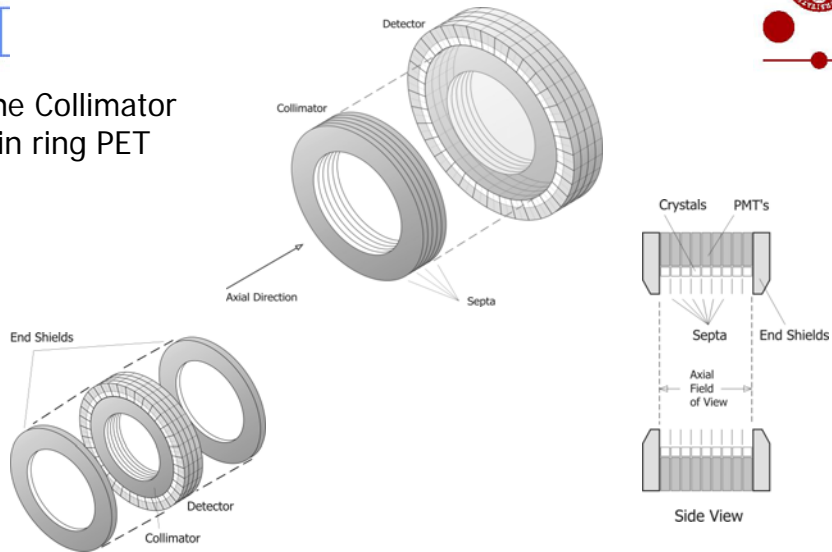
Interpolation needed before reconstruction



The sampled LORs are not equidistant, but become closer towards the edges.

The projections must be resampled prior to or during reconstruction

## The Collimator in ring PET

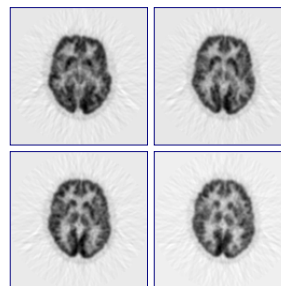


\$2018

53

## Static Frame Acquisition

- Set of slices in a single FOV
- No patient table motion
- Brain scan, tumor spot, heart examinations (myocardial perfusion, metabolism and viability)



Adjacent brain PET static slices

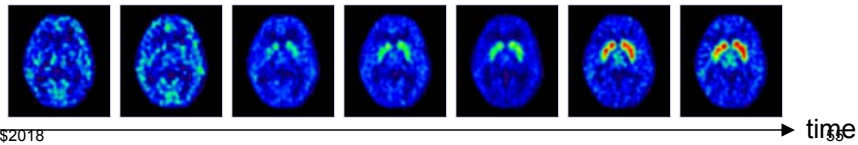
\$2018

54

## Dynamic Frame Acquisition

- Set of slices over time in a single FOV (like a movie)
- No patient table motion
- Start data acquisition as the tracer is administered
- Quantitative flow study (blood or other fluid): brain or heart

Cerebral dynamic PET scan  
Tracer is  $^{18}\text{F}$ -labeled D2 dopaminergic receptor ligand  
Finding: caudate and putamen normal tracer uptake



©2018

## Gated Acquisition

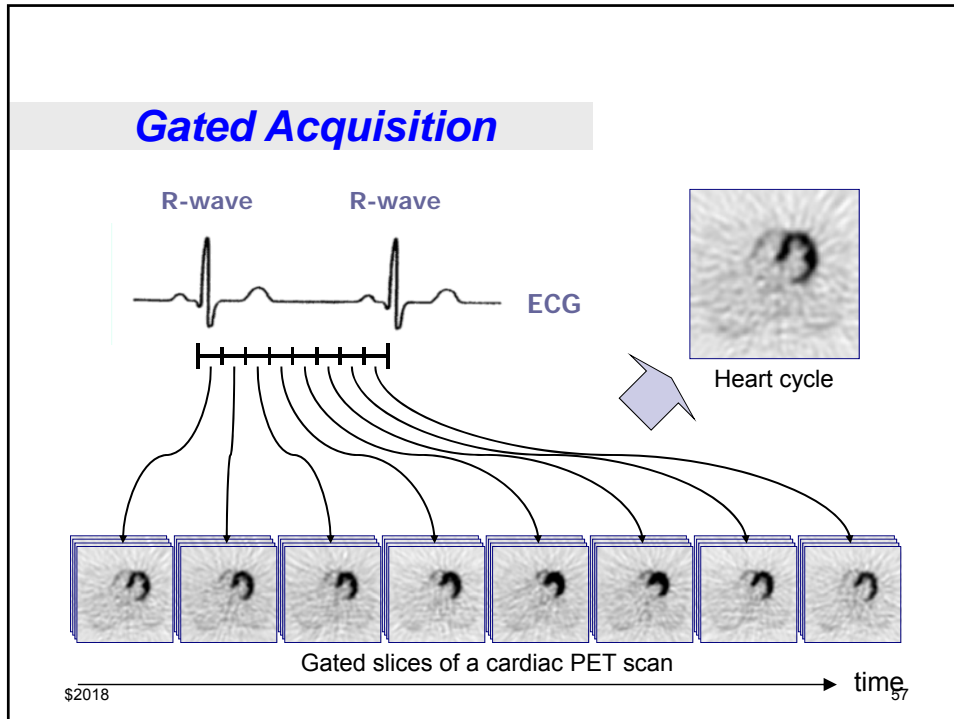
- Set of slices over time in a single FOV (like a movie)
- No patient table motion
- Heart imaging without cardiac motion blurring
- Myocardial perfusion, metabolism and viability



Electrocardiogram

©2018

56







## List Mode data (LM)

- List mode is an alternative way to store data during acquisition
- In the sinogram, events are counted in each matrix element. In List Mode, the two addresses (the detector numbers) of the two detectors involved are written to a continuous datastream.
- Every millisecond a timestamp is added to the stream
- Signals from cardiac or respiratory monitoring may be added

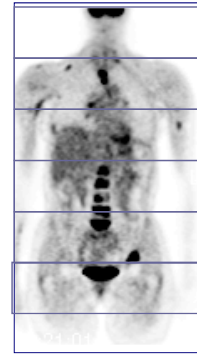
  

- After the acquisition, the LM-file can be replayed and sorted into sinograms
- This allows dynamic and gated studies to be acquired without assumptions about time frames and number of gating bins
- In some cases it may even save raw data storage capacity

\$2018 58

## Whole-Body Acquisition

- Set of slices in multiple FOVs
- Step-by-step tabletop motion during acquisition
- Metastatic spread of cancer

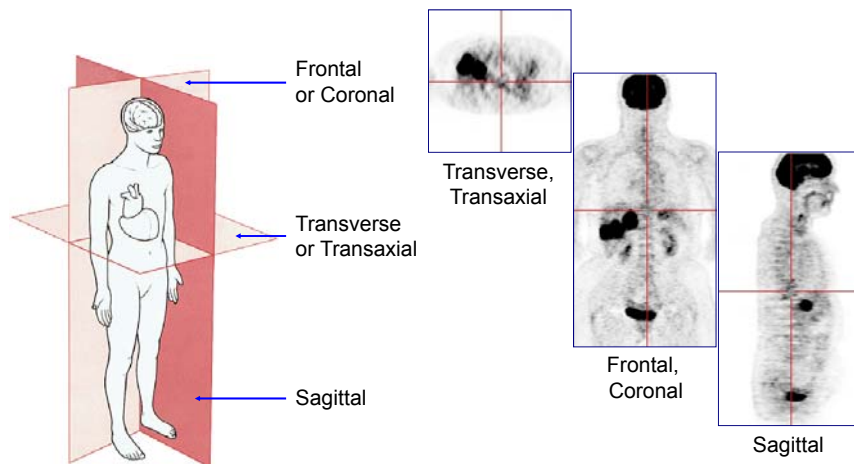


Whole-body scan 59

\$2018

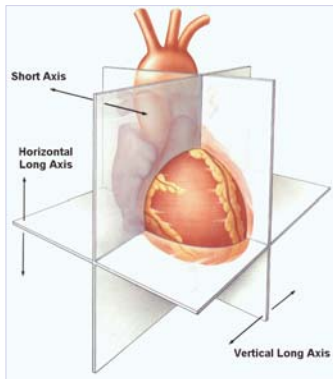


## Body Tomographic Planes

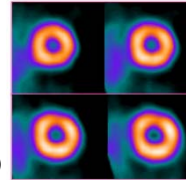


60

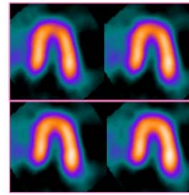
## Tomographic Planes for the Heart



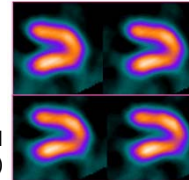
Short Axis (SA)



Horizontal Long Axis (HLA)



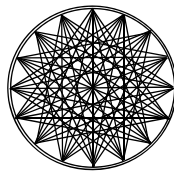
Vertical Long Axis (VLA)



\$2018

61

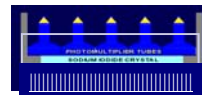
## Comparison of PET and SPECT:



all directions simultaneously

### + PET

- 1: Higher sensitivity, with "electronic collimation"
- 2: Fast dynamic scans
- 3: "Biological" tracers with C-11, N-13, O-15, F-18
- 4: Quantitative technique, with attenuation correction



én retning ad gangen

### + SPECT

- 1: Dual isotopes possible
- 2: Tc-99m generator + kits !
- 3: Less expensive to run

\$2018

62

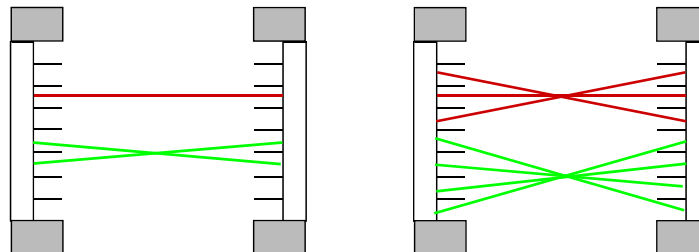


## Overview (4):



- Different kinds of tomography – PET in particular
  - Reconstruction from projections, FBP vs. iterative methods
  - Positron imaging history
  - Raw data structure - sinograms - types of acquisition and presentation
  - 2D/3D, advanced data structure – Michelogram
- 
- Resolution and noise
  - Scanner physics 1 – PET detectors
  - Scanner physics 2 – good, bad, and noise equivalent counts (NEC)
  - Attenuation and scatter correction of PET-data
  - Hybrid systems – PET/CT- PET/MR - SPECT/CT... Future ideas

## 2D Imaging



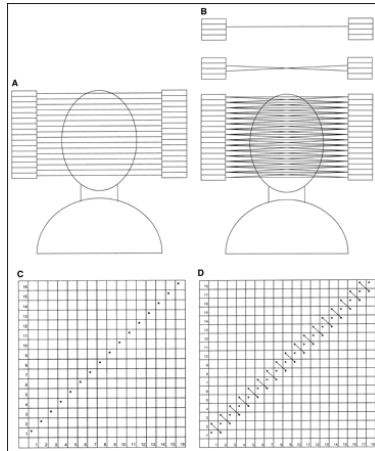
**High Resolution Mode**

- Direct  $\Delta Z = 0$
- Cross  $\Delta Z = \pm 1$
- Limited Sensitivity

**High Sensitivity Mode**

- Direct  $\Delta Z = 0, \pm 2$
- Cross  $\Delta Z = \pm 1, \pm 3$
- Increased Sensitivity

## Michelogram – direct and cross slices



The diagram shows all possible combinations of two detector rings.

The ones "allowed" are marked with a "\*".

Combinations that add to one sinogram are connected with a line between the points

Shown examples are the simple **direct slices** (diagonal in diagram) and simple **cross slices**

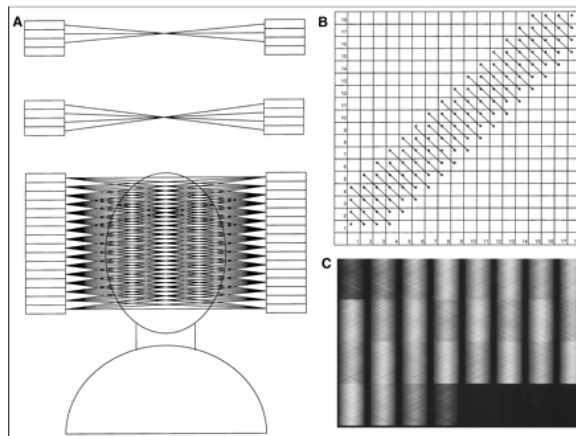
Direct only

Direct and Cross

\$2018

65

## Michelogram – 2D "span 7"



The number of combinations involved in direct and cross slices is known as the "**SPAN**"

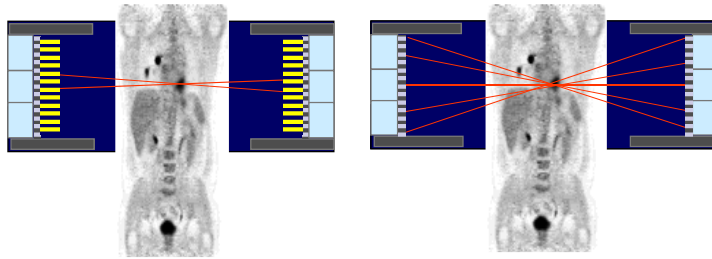
-in this case 7

Note how the sensitivity decreases towards the edge of the axial Field-of-View

\$2018

66

## 2D / 3D

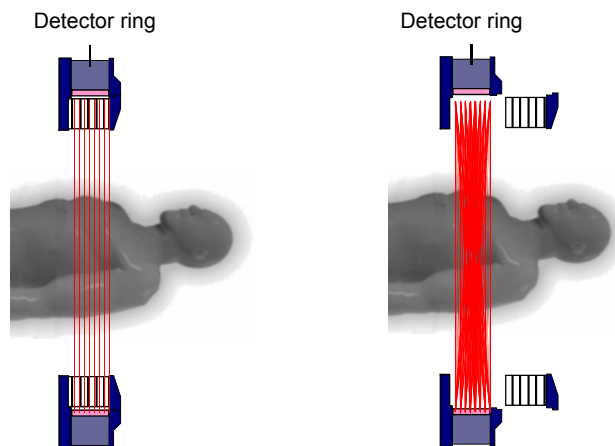


**2D ACQUISITION MODE**  
 septa employed  
 low acceptance solid angle

**3D ACQUISITION MODE**  
 no septa  
 High(er) acceptance solid angle

*[NOT used anymore]*

## 2D/3D Volume Acquisition



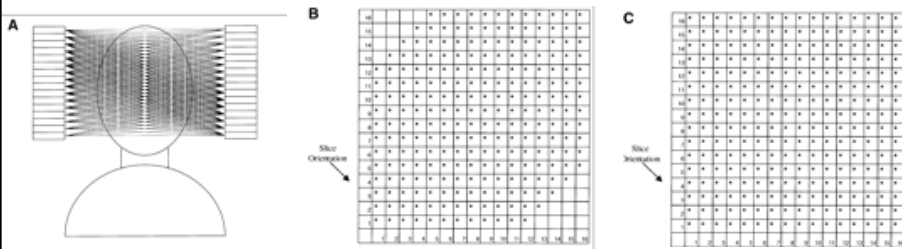
2D acquisition  
 (Septa installed)

3D acquisition  
 (Septa removed)

# Michelogram – 3D, RD11 and RD15

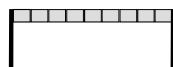


RD = Ring Difference



In 3D, where larger angles (ring differences) are allowed, the michelogram becomes populated further away from the diagonal – eventually completely filled.

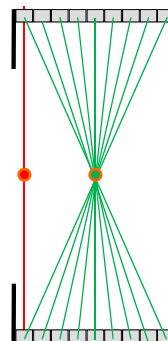
# Sensitivity in "3D" is position dependent



3D mode

There is a large difference between center and edge slices due to the number of LORs that contribute

The "ideal" triangle is most often truncated like this:  
(we are not allowing all angles)



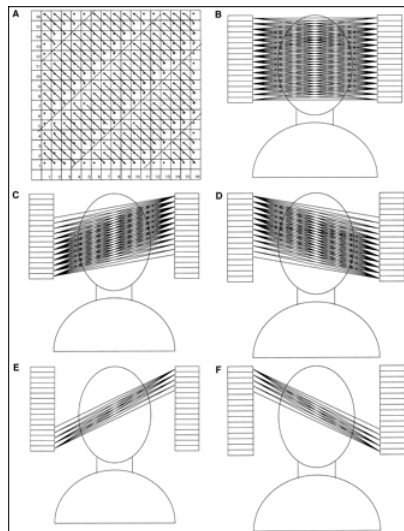
3D mode

- and therefore we need "overlap" in whole-body scanning



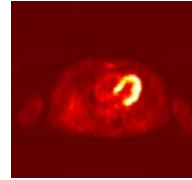
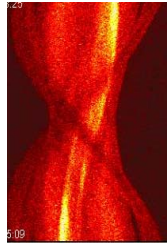
The overlapping scans add up to give a constant sensitivity and noise level (except for top and bottom)

### 3D data – span 7



Also for 3D, points in the michelogram may be joined, reducing the number of sinograms stored.

## Image Reconstruction



- Filtered Back-Projection methods:
  - 2D Filtered Back-Projection (2D FBP)
  - 3D Filtered Back-Projection (3D FBP)
- Iterative Reconstruction methods:
  - Maximum Likelihood Expectation Maximization (ML-EM)
  - Ordered Subsets Expectation Maximization (OSEM)
  - Full 3D iteration



## Overview (5):

- Different kinds of tomography – PET in particular
  - Reconstruction from projections, FBP vs. iterative methods
  - Positron imaging history
  - Raw data structure - sinograms - types of acquisition and presentation
  - 2D/3D, advanced data structure – Michelogram
- 
- Resolution and noise
  - Scanner physics 1 – PET detectors
  - Scanner physics 2 – good, bad, and noise equivalent counts (NEC)
  - Attenuation and scatter correction of PET-data
  - Hybrid systems – PET/CT- PET/MR - SPECT/CT... Future ideas

## FAQ #1:

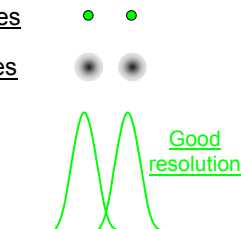
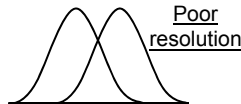
What is the smallest *[something]*  
you can see in a PET scanner?

Wrong question /No simple answer  
Depends on the activity concentration/contrast

## Spatial Resolution

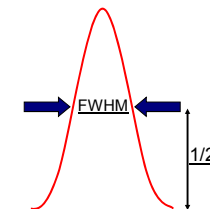
~~• How small an object  
can you see in PET?~~

■ Ability to separate two  
objects close  
together: **Resolution**



Line profile of a point source (PSF)

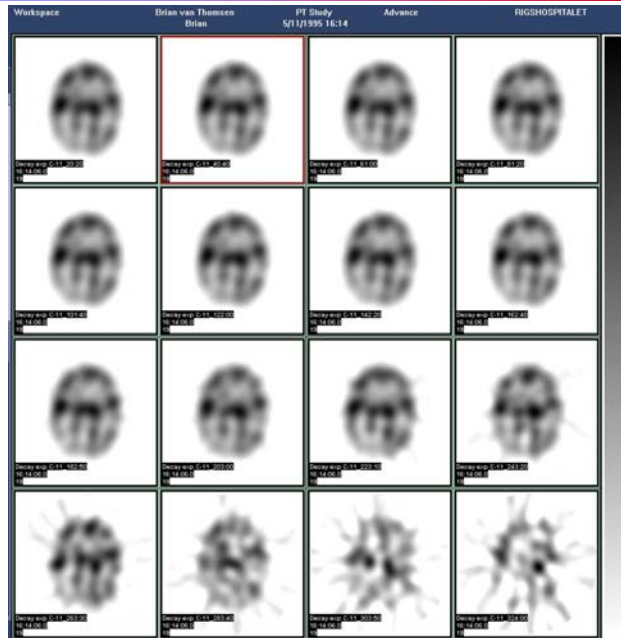
- Full Width at Half Maximum (FWHM) is the measure of resolution (unit: mm).
- Depends on position and direction in the field.
- Typical PET resolution: FWHM  $\approx$  5 mm.



Filtering is a balance between noise and resolution (FWHM)

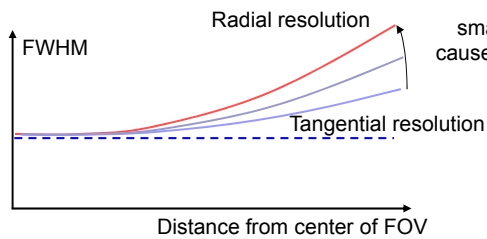
20 mm

\$2018



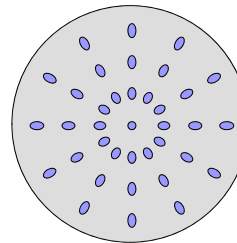
77

## Radial Vs Tangential Resolution



smaller ring diameter cause more degradation

Plot of resolution versus radial position



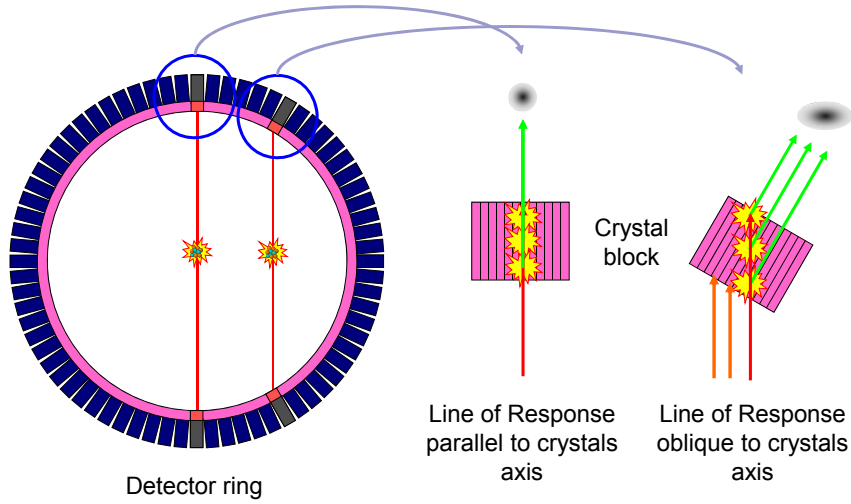
Smearing of point sources within the FOV

- Radial resolution degrades toward the edge of the field-of-view.
- Tangential resolution is almost constant within the field-of-view.

\$2018

78

# Radial Vs Tangential Resolution

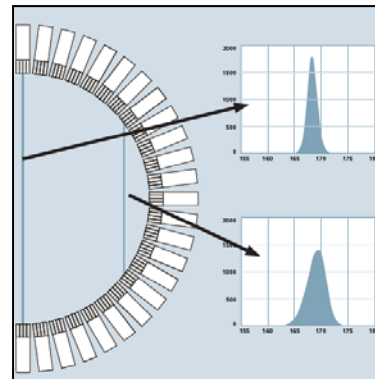
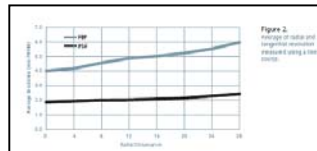


\$2018

79

# Results of modeling PSF in reconstruction

(example: Siemens "High definition" recon)



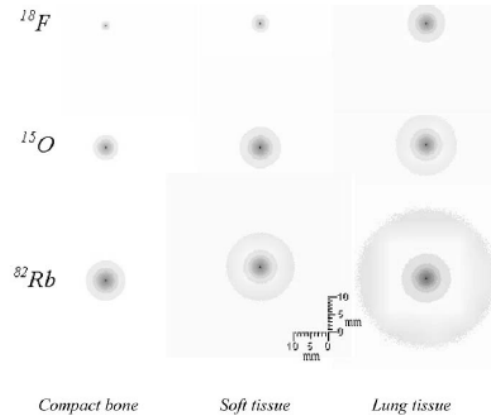
\$2018

80

## Positron flight in human tissues

Sanchez-Crespo A et al. Eur J Nucl Med Mol Imaging (2004)

Fig. 1. Monte Carlo-calculated distribution of annihilation events around a positron point source embedded in different human tissues as seen in the image plane of a PET camera

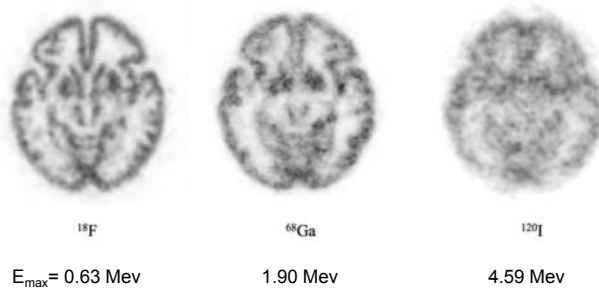


\$2018

81

## Effect of positron energy

lida-phantom

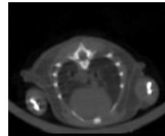


\$2018

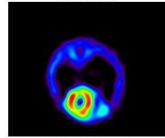
82

## Mouse Heart PET/CT: 28g Mouse

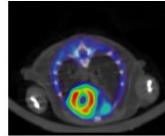
Image courtesy of David Stout  
Crump Institute for Molecular Imaging, Los Angeles CA



microCAT

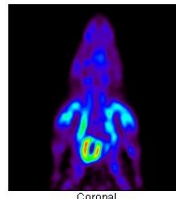


microPET Transverse

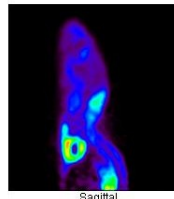


Fused PET-CT

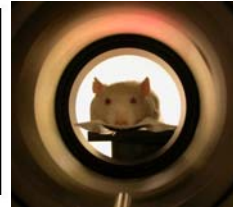
microPET® Focus™220 Mouse FDG Images  
Living mouse, non-gated



Coronal



Sagittal



Similar devices have been installed at the Panum Institute

\$2018

83



## Overview (6):

- Different kinds of tomography – PET in particular
  - Reconstruction from projections, FBP vs. iterative methods
  - Positron imaging history
  - Raw data structure - sinograms - types of acquisition and presentation
  - 2D/3D, advanced data structure – Michelogram
- 
- Resolution and noise
  - Scanner physics 1 – PET detectors
  - Scanner physics 2 – good, bad, and noise equivalent counts (NEC)
  - Attenuation and scatter correction of PET-data
  - Hybrid systems – PET/CT- PET/MR - SPECT/CT... Future ideas

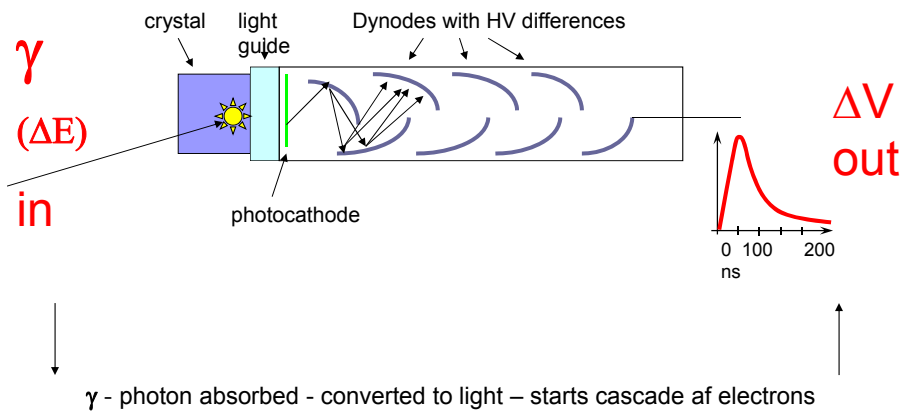
\$2018

84

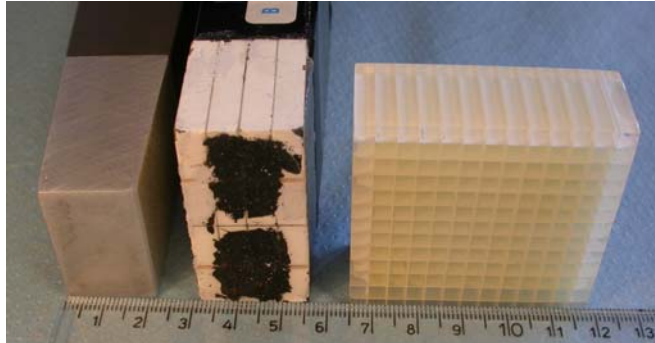
## Detection of 511 keV photons

- First, we need to stop the photons
  - That requires some high Z, high density material
  - which converts the energy to low energy photons
  
- Then this signal must be amplified and digitized
  - Two options:
    - photo multiplier tube (PMT) or
    - solid state detectors (APD, SiPM)

## Scintillation detector



## Evolution of PET-detectors



**Therascan**  
1981 (89)  
single detector  
20\*35 mm  
total # 256

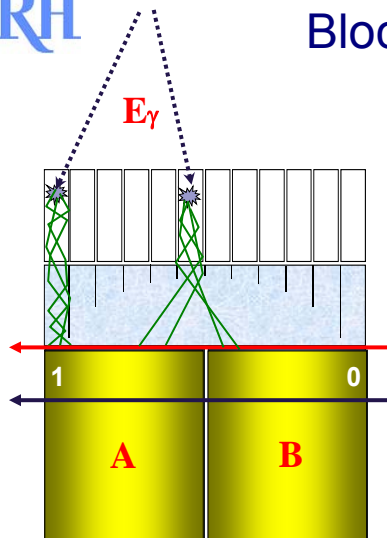
**4096+**  
1991  
4\*4 block  
6\*12 mm  
total # 4096

**Biograph Hirez**  
2005  
13\*13 block  
4\*4 mm  
total # 24336

\$2018

87

## Block Concept



$$X = A / (A + B)$$

$$X_1 \quad X_1 = 100 / (100 + 0) = 1.0$$

$$X_2 \quad X_2 = 55 / (55 + 45) = 0.55$$

\$2018

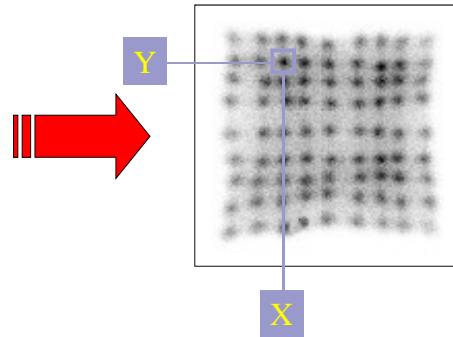
88

## Flood Histogram / Position Map

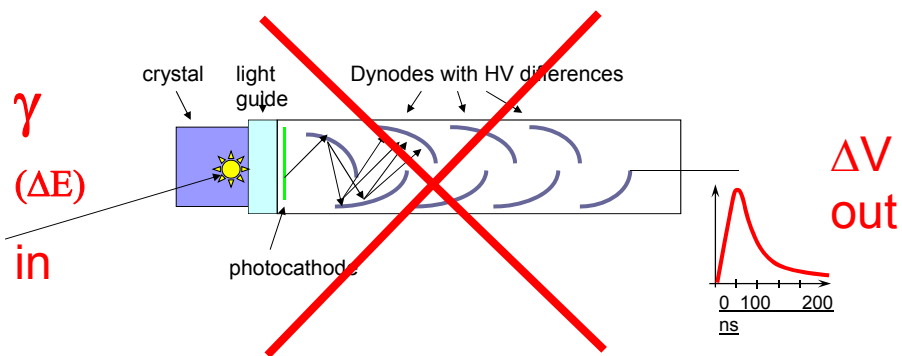
### Anger Logic

$$X = \frac{A}{A + B}$$

$$Y = \frac{C}{C + D}$$



## Scintillation detector



γ - photon absorbed - converted to light - starts cascade of electrons

**Not effective in a MAGNETIC FIELD !**

Solid-state photo-multipliers (SSPMs) can be fabricated from small silicon sub-pixels to replace PMTs making them attractive for **PET+MR and TOF-PET**:

- fast, low-jitter time response
- magnetic field immunity
- small form-factor

**Technical challenges:**

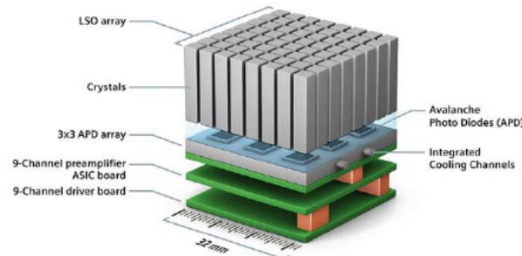
- Readout circuits/ASIC development
- Multiplexing options
- Handling multi-crystal events
- MR compatible architecture

	PMT	SSPM SiPM	APD
Detection efficiency	25%	50%	50%
Coincidence timing res.	550ps	250ps	1000ps
Gain	$10^6$	$10^5$ - $10^6$	$10^2$
Height	100 mm	2 mm	2 mm
Magnetic Sensitivity	High	Low	Low
Noise	Low	Low	High
Cost	Low	High	High



GE imagination at work  
\$2018

91

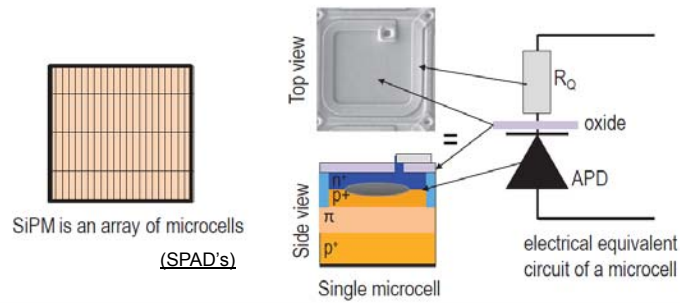


\$2018

92

# SiPM = Silicon PhotoMultiplier

## SiPM structure



Copyright © Hamamatsu Photonics K.K. All Rights Reserved 6

First characterization of a digital SiPM based time-of-flight PET detector with 1 mm spatial resolution 3063

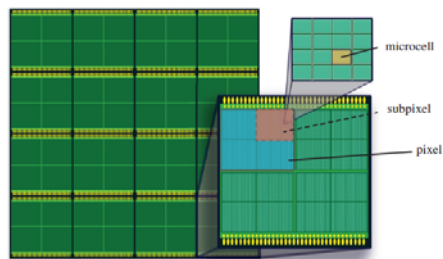
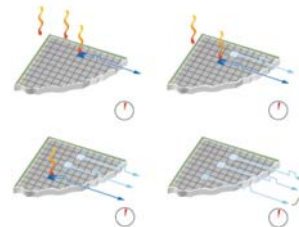


Figure 1. Schematic representation of the digital silicon photomultiplier (dSiPM) array. The larger inset depicts a zoom on a single die consisting of four pixels. Each pixel contains 6396 microcells (a number of which are shown in the smaller insets) that are arranged into 4 subpixels.

- 1 Tile
- 16 dies
- 4 pixels
- 4 subpixels
- ~1600 microcells

## Philips Vereos Digital PET dSiPM



# DOI measurement with APD

(Depth of Interaction – to avoid parallax-errors)

**Parallax error: continuous DOI measurement**

**Differential measurement DUALAPD**

**Differential measurement SiPD-PMT**

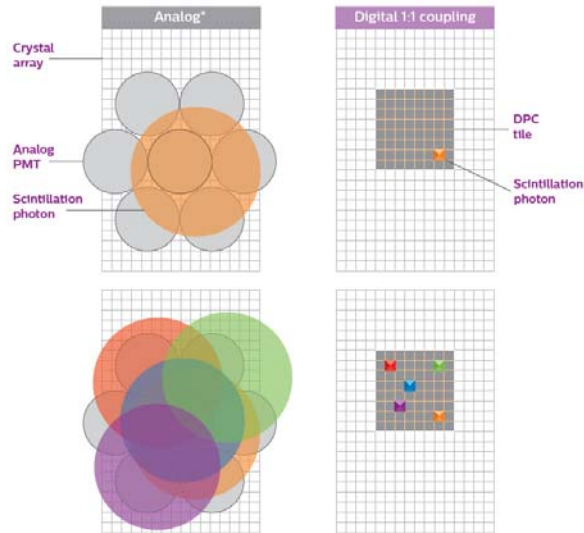
Resolution DOI measurement: 3 mm FWHM

An LSO scintillator array for a PET detector module with depth of interaction measurement

- The PMT (single anode) provides the timing
- The SiPD (8x8) detects the crystal
- The ratio SiPD/(SiPD+PMT) returns the DOI

Presented at EANM 2008 by A. Del Guerra

# Shared PMTs versus 1 to 1 coupling



# PET Detector Components

Crystal elements  
and photomultiplier  
tubes



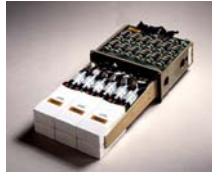
Detector  
ring

Detector block



Module  
array

Detector blocks  
and front-end  
electronics



Detector module

©2018

97

# PET (example: GE Advance)



PMT-gain

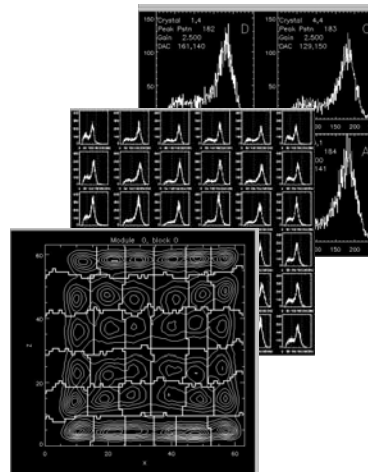
=

Energy-  
windows

336 \*



Uniformity

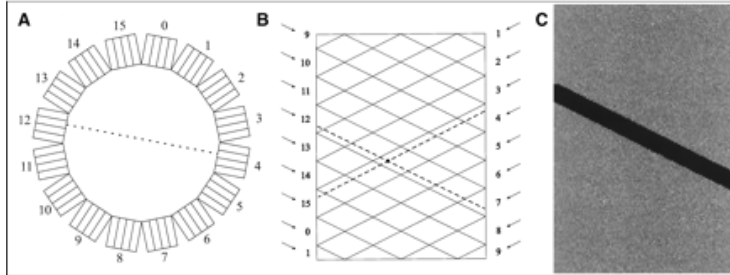


Every pair of blocks is tuned for coincidence timing

©2018

98

## Block contribution to sinogram



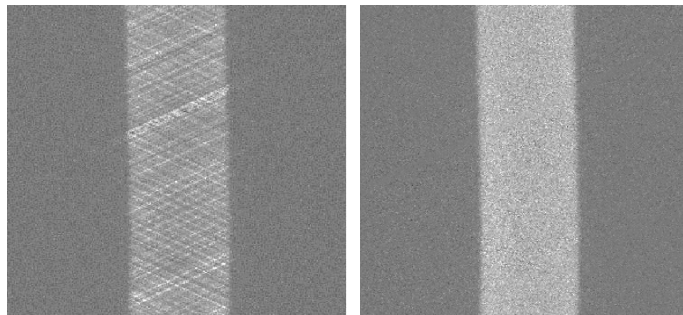
All the contributions from a single detector will be on a line, angled as shown. Due to sensitivity differences a certain "rhombic" structure will be visible in the sinogram.

One defective block will show up as a black, empty area in the sinogram



## Normalisation correction

- Compensates systematic efficiency variations (system geometry, crystal efficiency)



Sinogram **before** normalisation correction

Sinogram **after** normalisation correction

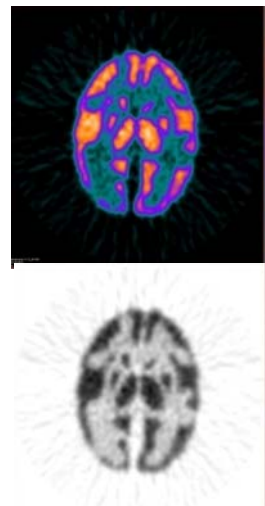
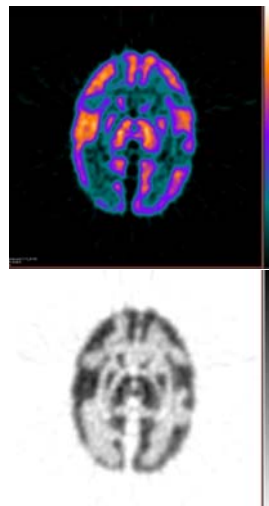
## Siemens Biograph uses $^{68}\text{Ge}$ cylinder



\$2018

101

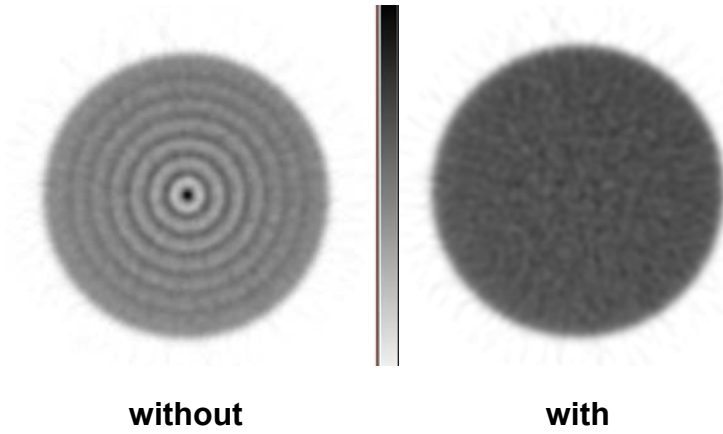
## Effect of Normalisation



\$2018

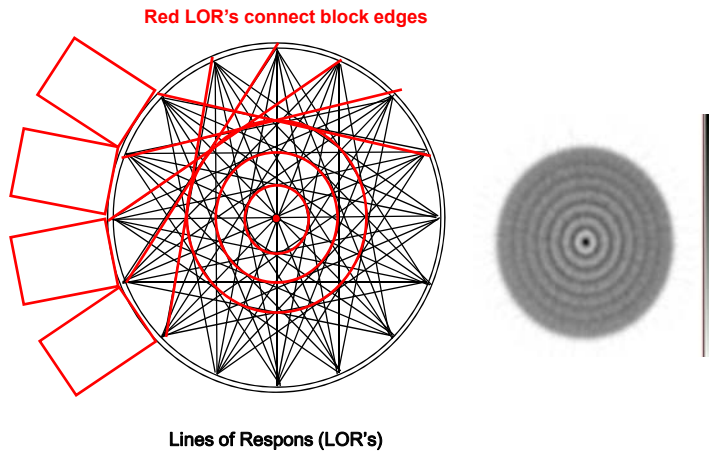
102

# Uniform phantom – very sensitive to NORM



# Normalisation

(digression on the origin of ring artefacts)



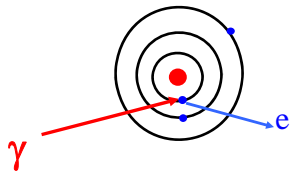


## Overview (7):

- Different kinds of tomography – PET in particular
  - Reconstruction from projections, FBP vs. iterative methods
  - Positron imaging history
  - Raw data structure - sinograms - types of acquisition and presentation
  - 2D/3D, advanced data structure – Michelogram
- 
- Resolution and noise
  - Scanner physics 1 – PET detectors
  - Scanner physics 2 – good, bad, and noise equivalent counts (NEC)
  - Attenuation and scatter correction of PET-data
  - Hybrid systems – PET/CT- PET/MR - SPECT/CT... Future ideas

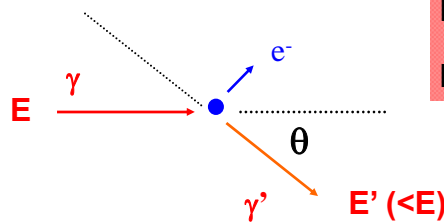
## Two processes stop photons in tissue:

### Absorption:

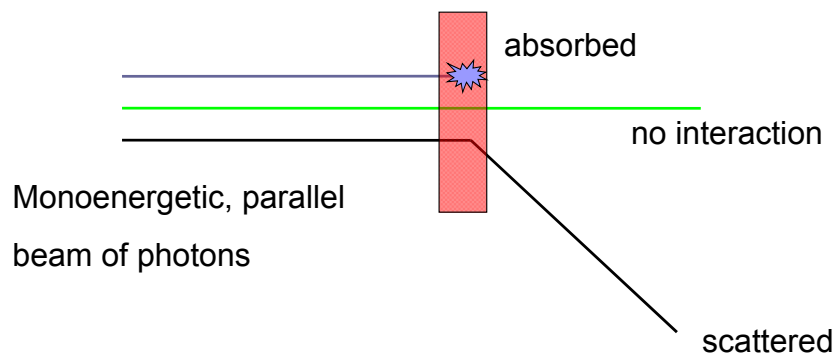
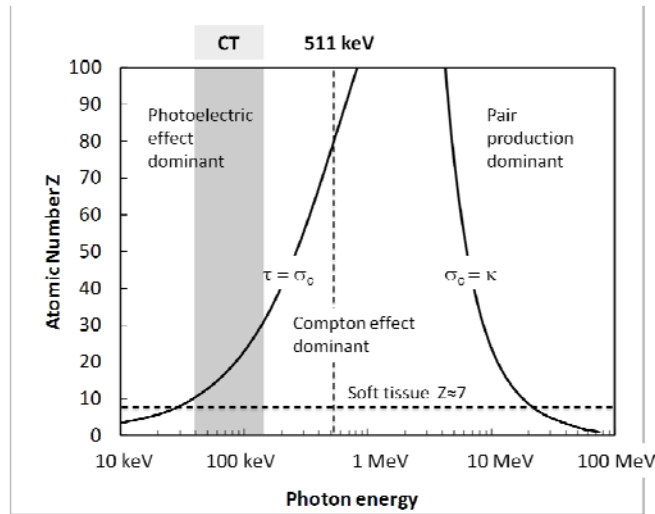


Simple,  
no parameters

### Compton scattering:

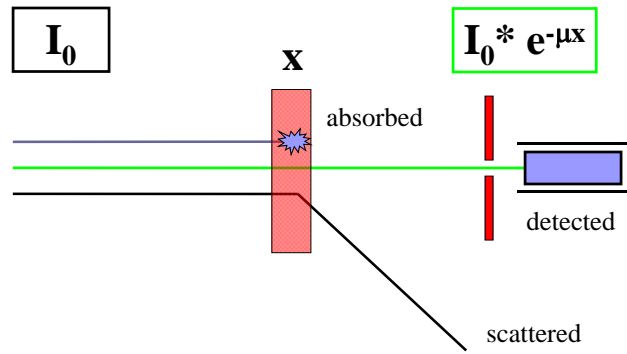


Parameters  
E' and  $\theta$



$$\text{Attenuation} = \text{Absorption} + \text{Scatter}$$

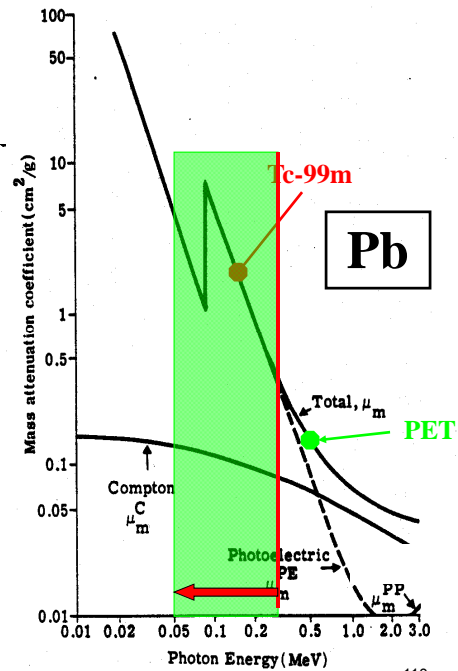
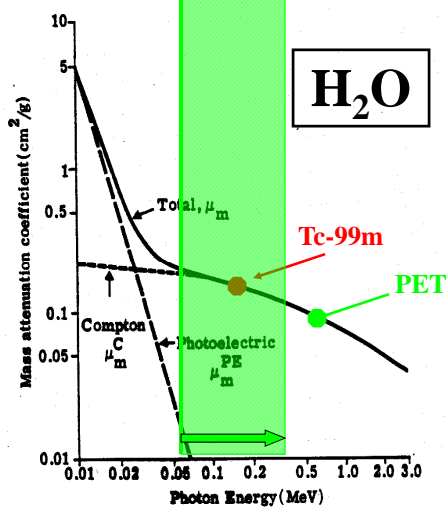
Linear attenuation coefficient:  $\mu$



Attenuation = Absorption + Scatter

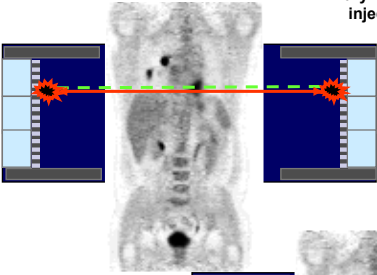
$$\mu_{\text{total}} = \mu_{\text{abs}} + \mu_{\text{scatter}}$$

Mass attenuation coefficients in water (soft tissue) and lead



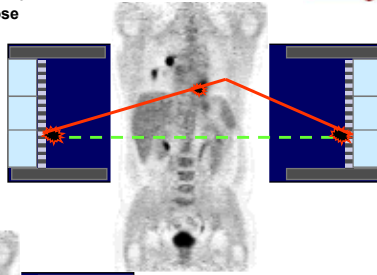
**RH** 

Trues Coincidence

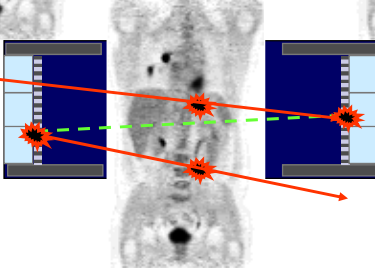


Vary linearly with injected dose

Scatter Coincidence



Vary linearly with injected dose



Random Coincidence

Vary quadratically with injected dose and linearly with coincidence window

Not all counts are created equal...

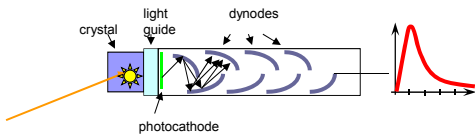
there are the good, the bad, and the ugly counts

\$2018
111

**RH** 

## The ideal scintillation detector has

- High element no (Z) ⇒ Good absorption
- High density ( $\rho$ ) ⇒ High sensitivity
  
- Short decay of light ⇒ Less Deadtime, fast counting
- High light output ⇒ Narrow coincidence window  
⇒ less Randoms
- Low price ⇒ Good energy resolution  
⇒ Scatter rejection



\$2018
112

## PET Detector Scintillator Materials



Crystal material	max Z	effective Z	density g/cm <sup>3</sup>	output photons/keV	decay time ns
Nal:Tl	53	51	3.7	40	230
BGO	83	73	7.1	8	300
LSO:Ce	71	66	7.4	28	40
LYSO	71	54	5.4	28	53
GSO:Ce	64	59	6.7	7.5	56
BaF <sub>2</sub>	55	54	4.1	2	0.8

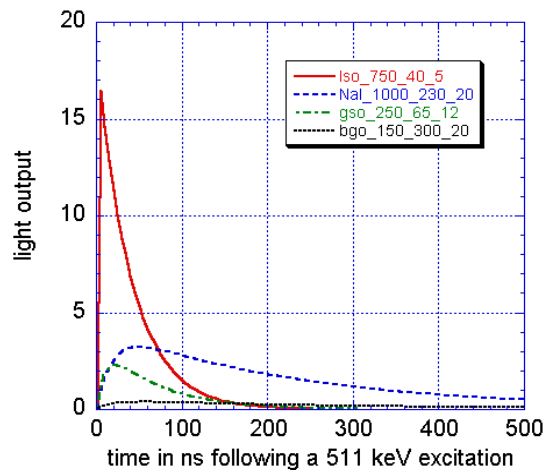
"New" promising crystal materials: LaBr<sub>3</sub>, CeBr<sub>3</sub> and TlBr

BGO may have a come-back

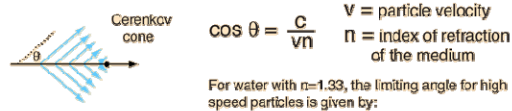
## Scintillator Light Output



Light fractions emitted during the first 100 ns:  
LSO 92%; Nal 35%; GSO 79%; BGO 28%



# Cerenkov photons



For water with  $n=1.33$ , the limiting angle for high speed particles is given by:

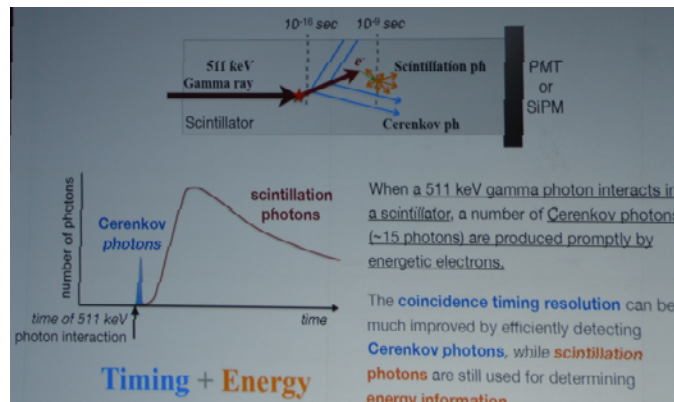
$$\theta = \cos^{-1} \frac{1}{1.33} = 41.2^\circ$$

The threshold particle speed for Cerenkov radiation is  $v = c/n$ , which for an electron in water gives a threshold particle kinetic energy of 0.26 MeV.

$$\beta = 0.752, E_{\text{electron}} = \gamma m_e c^2 = \frac{1}{\sqrt{1 - \beta^2}} m_e c^2 = 1.52(0.511 \text{ MeV}) = .775 \text{ MeV}$$

$$\text{Kinetic energy} = 0.775 \text{ MeV} - 0.511 \text{ MeV} = 0.26 \text{ MeV}$$

# Timing with Cerenkov



Kwon et al, MIC 2016

# Noise Equivalent Counts (NEC)

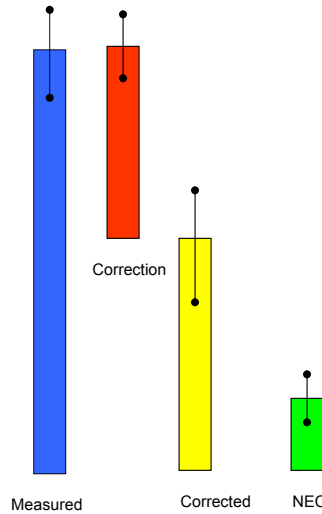


When correcting for randoms and scatter, counts are subtracted

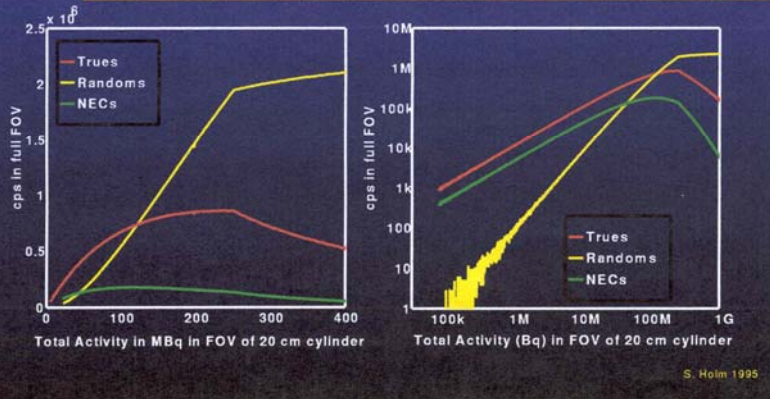
But the noise (uncertainty) is added!

The result is of less value than if the same #counts were measured directly

NEC is the number of GOOD counts to which the result is equivalent (i.e. same COV)



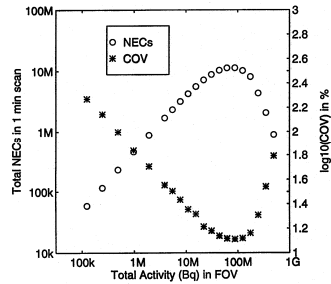
## NEC



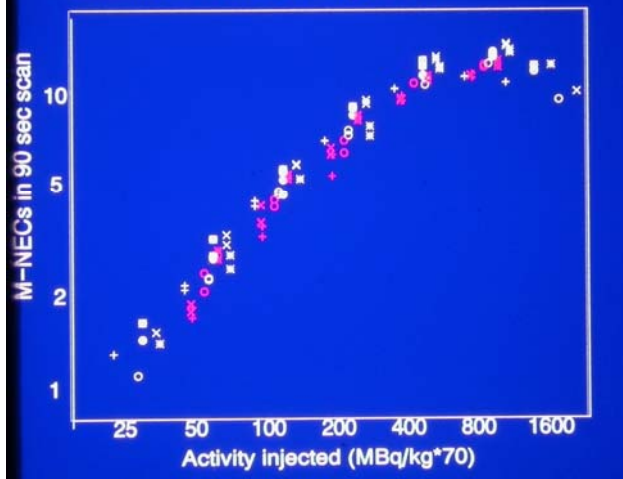
## Noise Equivalent Counts (or count rate)

$$SNR^2 = NECR \cdot \Delta t = \left[ \frac{T^2}{(P + kR)} \right] \Delta t = \left[ \frac{T^2}{(T + S + (k+1)R)} \right] \Delta t$$

- k = 0 (R is estimated from singles)
- K = 1 (R measured in delayed window)
  
- NEC actually "reflects" the noise!



## Noise Equivalent Counts Data from 112 Bolus injections



### Optimizing Injected Dose in Clinical PET by Accurately Modeling the Counting-Rate Response Functions Specific to Individual Patient Scans

Charles C. Watson, PhD<sup>1</sup>; Michael E. Casey, PhD<sup>2</sup>; Bernard Bendriem, PhD<sup>3</sup>; Jonathan P. Carney, PhD<sup>4</sup>;  
David W. Townsend, PhD<sup>5</sup>; Stefan Eberl, PhD<sup>6</sup>; Steve Meikle, PhD<sup>5</sup>; and Frank P. DiFilippo, PhD<sup>7</sup>

J Nucl Med 2005; 46:1825-1834

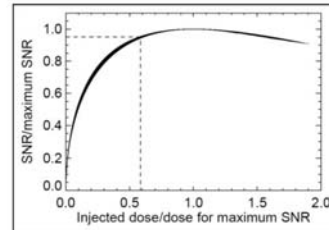
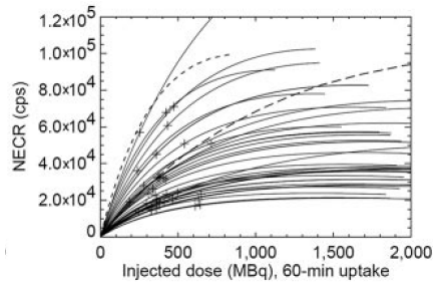
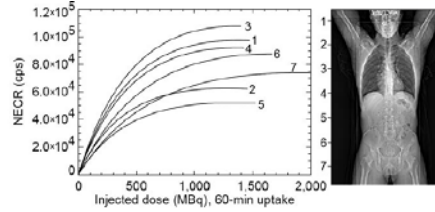


FIGURE 3. Relative response curves for 163 scans on conventional LSO PET/CT scanner, obtained by scaling SNR (1 $\sigma$  case) and  $D_{95}$  by their values at peak response.

\$2016

121

## Time to breath...



[Reykjavik, 25. August 2011\$]

\$2018

122



## Overview (8):

- Different kinds of tomography – PET in particular
  - Reconstruction from projections, FBP vs. iterative methods
  - Positron imaging history
  - Raw data structure - sinograms - types of acquisition and presentation
  - 2D/3D, advanced data structure – Michelogram
- 
- Resolution and noise
  - Scanner physics 1 – PET detectors
  - Scanner physics 2 – good, bad, and noise equivalent counts (NEC)
  - Attenuation and scatter correction of PET-data
  - Hybrid systems – PET/CT- PET/MR - SPECT/CT... Future ideas

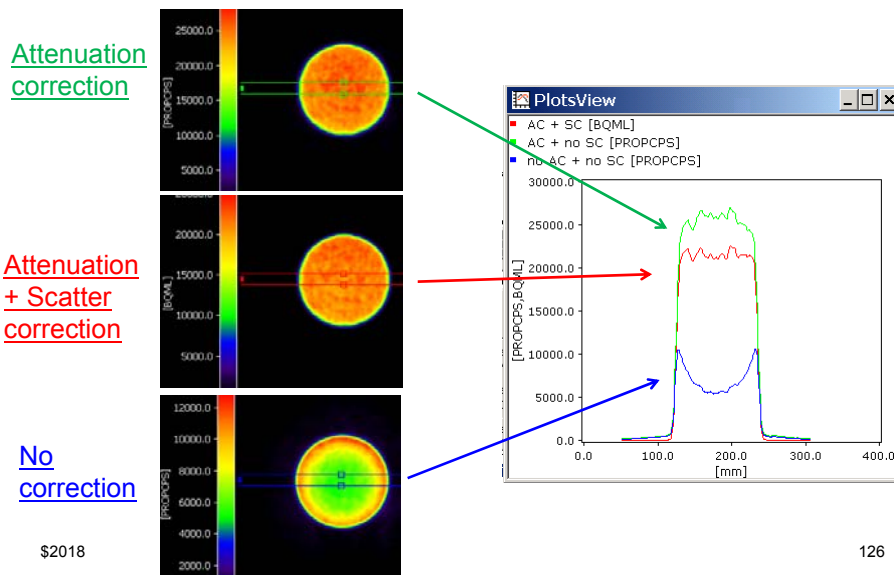
## PET is a quantitative technique

(although most people don't care these days...)

IF all the necessary corrections are applied:

- Deadtime
- Geometry, Normalization
- Randoms subtraction
- Attenuation and scatter
- Decay
- ...

- It is a paradox in our terminology that from a *physics* point of view, **attenuation** (in NM) is caused mainly by **scattering** processes (and only partly by absorption)
- but in our *correction* procedures:
  - **Attenuation** is "lack of counts" that we must restore while
  - **Scatter** is a surplus of counts (in wrong places) to be removed
- Correcting one without the other will give wrong results

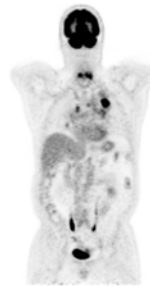


## Attenuation correction

- Provides PET images closer to real radiotracer distribution
- Corrects attenuation-introduced geometric artifacts
- Improves lesion detection in deep organs
- Allows absolute quantitative PET studies



Without attenuation correction



With attenuation correction

\$2018

127

## Anthropomorphic phantom

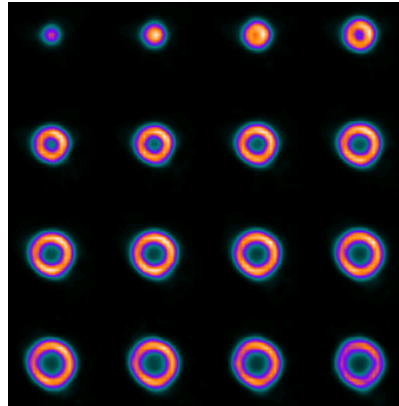
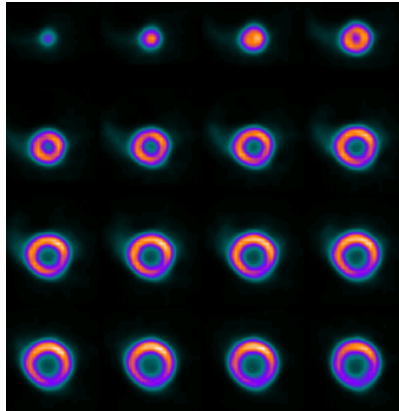


\$2018

128

BEFORE Correction

AFTER Correction



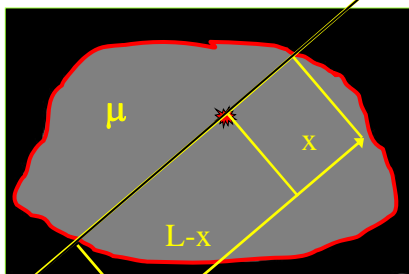
Conclusion: Correction may cure the patients...(?)

\$2018

129

Attenuation Correction

$$P_1 = \exp(-\mu x)$$

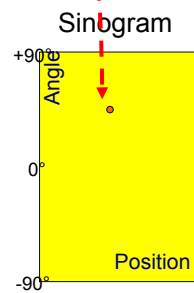


$(r, \theta)$

$L(r, \theta)$

$$P_2 = \exp(-\mu(L-x))$$

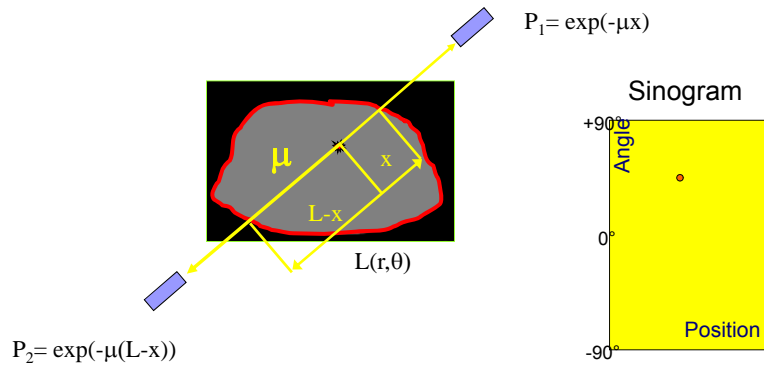
\$2018



130

Probability of a coincidence:

$$P(r,\theta) = P_1 * P_2 = \exp(-\mu x) * \exp(-\mu(L-x)) = \exp(-\mu L) \text{ [independent of } x \text{ !]}$$



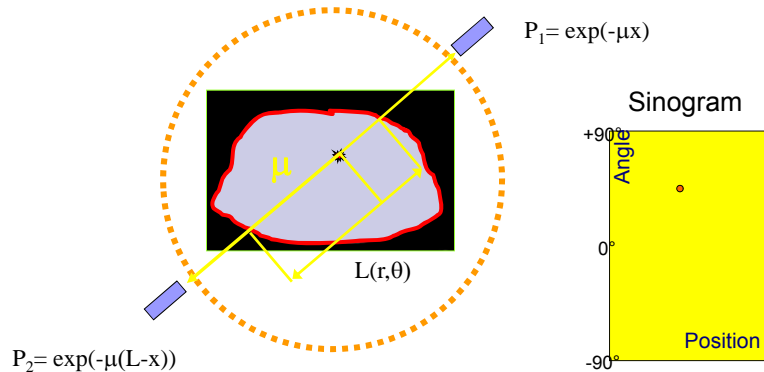
\$2018

131

Probability of a coincidence:

$$P(r,\theta) = P_1 * P_2 = \exp(-\mu x) * \exp(-\mu(L-x)) = \exp(-\mu L) \text{ [independent of } x \text{ !]}$$

- and therefore easily measured with external (rotating) pin/point source
- and corrected: each line of response multiplied by its own  $\exp(\mu L)$



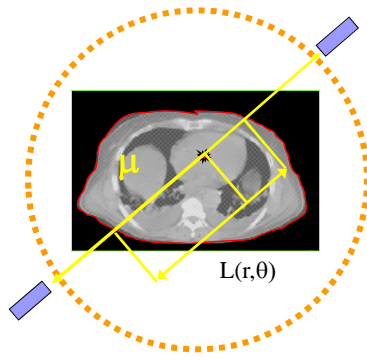
\$2018

132

If  $\mu$  is not a constant (and it IS NOT):

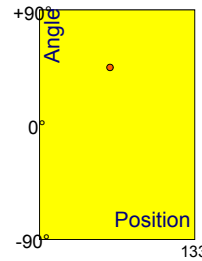
$$P_1 * P_2 = \exp\left(-\int_0^x \mu(x) dx\right) * \exp\left(-\int_x^L \mu(x) dx\right) = \exp\left(-\int_0^L \mu(x) dx\right)$$

still independent of the source position



$$P_1 = \exp\left(-\int_0^x \mu(x) dx\right)$$

Transmission Sinogram



$$P_2 = \exp\left(-\int_x^L \mu(x) dx\right)$$

\$2018

133

GE used  $^{68}\text{Ge}$  Pin sources



GE 4096 (by hand)



GE Advance and GE Discovery LS  
(3 pins, automated complex robotic arm)



GE Discovery ST etc.  
(1 pin in trunk)



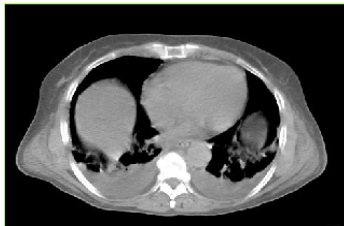
\$2018

134

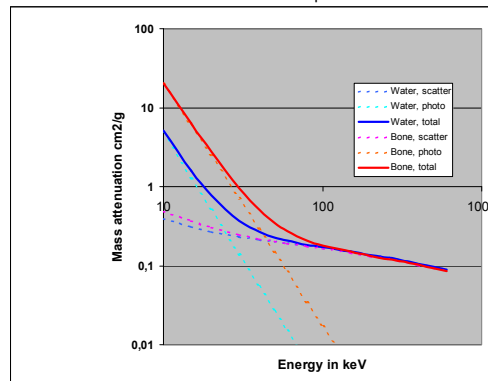
## CT scans are $\mu$ -maps (in HU)



They can be used for attenuation correction – essentially noise free  
 But:  $\mu(511 \text{ keV}) \neq \mu(80 \text{ keV})$ , therefore a scaling is required  
 Soft tissue and bone (and contrast) scale differently  
 Not one simple scaling factor, but a lookup table for  $\mu(\text{HU}; \text{kV}_p)$



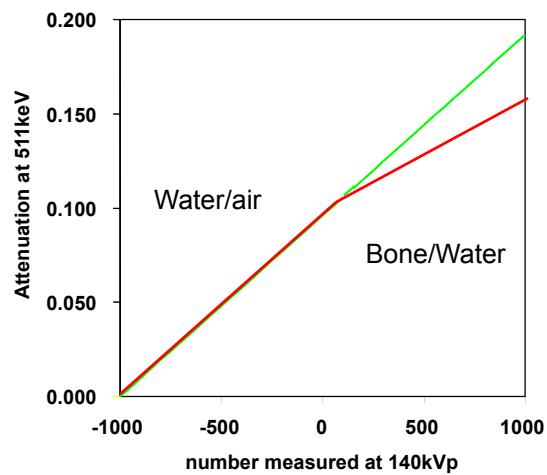
\$2018



## Conversion of CT Numbers to $\mu_{\text{PET}}$



- For CT values  $< 100$ , materials are assumed to have an energy dependence similar to water
- For CT values  $> 100$ , material is assumed to have an energy dependence similar to a mixture of bone and water
- The green line shows the effect of using water scaling for all materials



\$2018

136

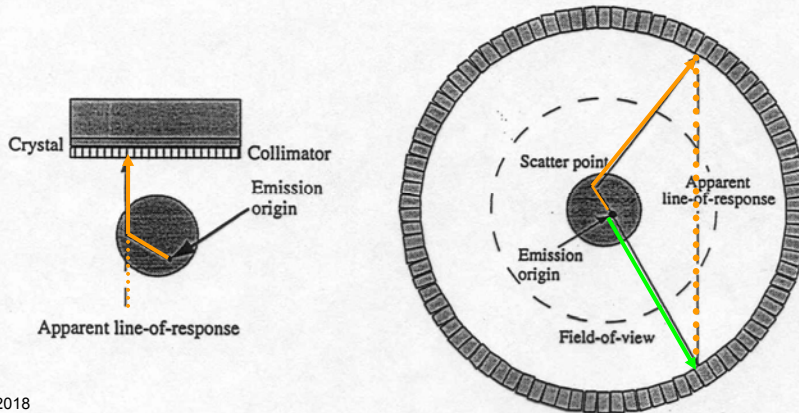
# Scatter in

## SPECT

## PET

appears "inside" the object

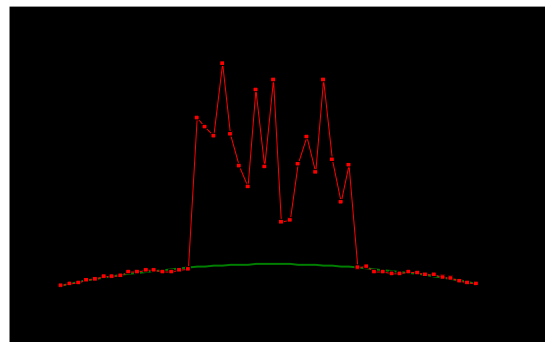
may appear outside object



\$2018

137

# Scatter Correction by Function Fitting



- Fit data to projection tails
- This requires tails!
- More elaborate methods model the scatter from detailed knowledge of the object

\$2018

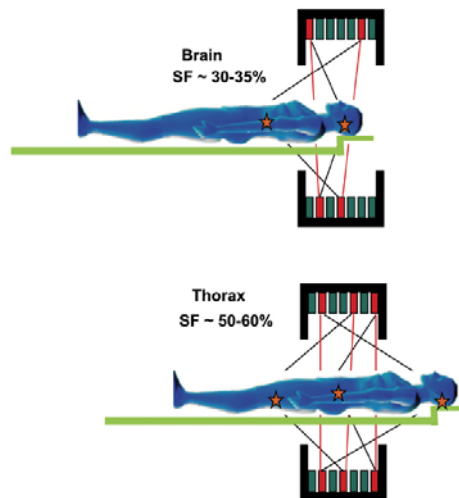
138

## Scatter correction techniques

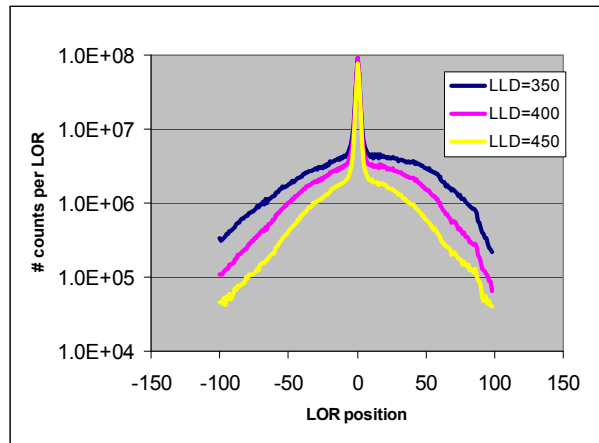


- Metz / Wiener filtering
- Asymmetrical energy window
- Dual energy window
- Dual photopeak window
- Weighing of detected events (WAM)
- Channel ratio method
- Photopeak energy distribution analysis
- Position dependent scatter correction
- Stationary / Non-stationary deconvolution
- Iterative reconstruction techniques
- Neural network
- Pixel by pixel spectral analysis
- Regularized deconvolution-fitting method
- Scatter-free imaging (CFI)
- Holopectral imaging
- Factor analysis of medical image sequences
- Single scatter simulation techniques**

## Scatter fractions in 3D PET

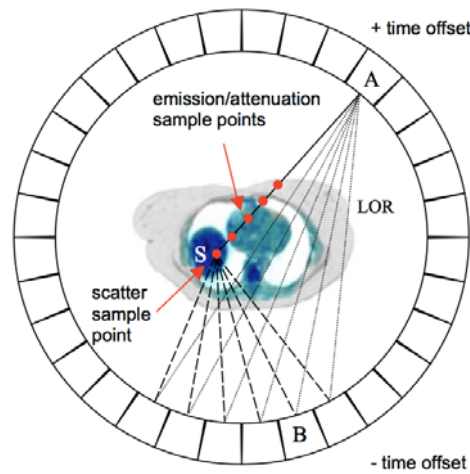


# Scatter removal by energy discrimination

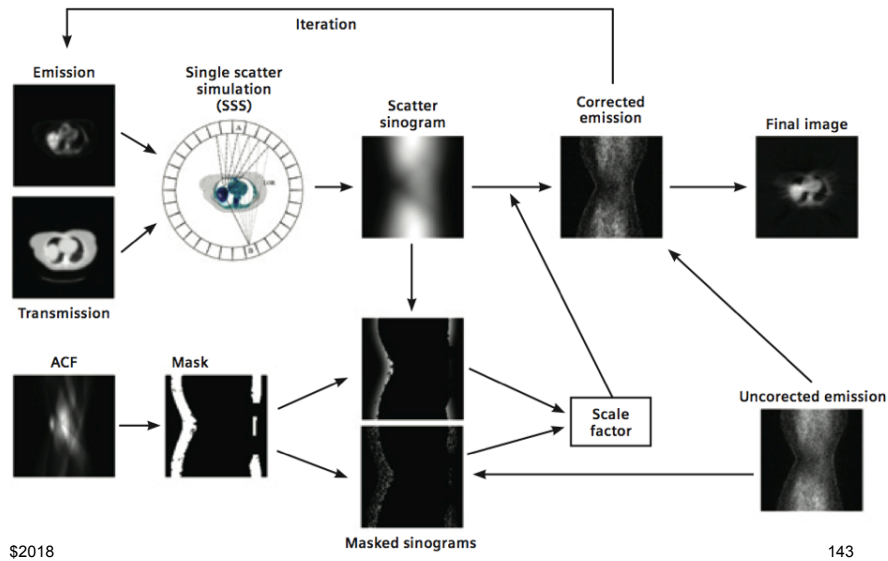


(keV)

# Scatter correction



# Scatter correction



# Overview (9):



- Different kinds of tomography – PET in particular
  - Reconstruction from projections, FBP vs. iterative methods
  - Positron imaging history
  - Raw data structure - sinograms - types of acquisition and presentation
  - 2D/3D, advanced data structure – Michelogram
- 
- Resolution and noise
  - Scanner physics 1 – PET detectors
  - Scanner physics 2 – good, bad, and noise equivalent counts (NEC)
  - Attenuation and scatter correction of PET-data
  - Hybrid systems – PET/CT- PET/MR - SPECT/CT... Future ideas

## Good reasons to combine PET and CT:

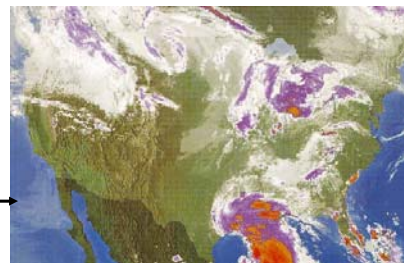


- 0: Because it was possible (*MR more difficult*)
- 1: Complementary information
  - structure + function
  - anatomy + physiologi/biochemistry
- 2: Exact localization ("free" coregistration)
- 3: Improved attenuation correction in PET

## Functional Images



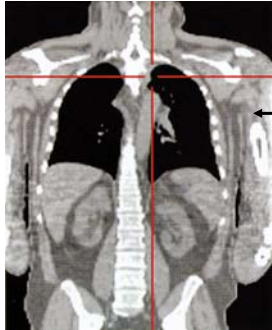
PET Images  
"abnormal activity"



Weather Patterns  
"weather activity"



## Structural Images



CT Images  
“precise body’s anatomy”



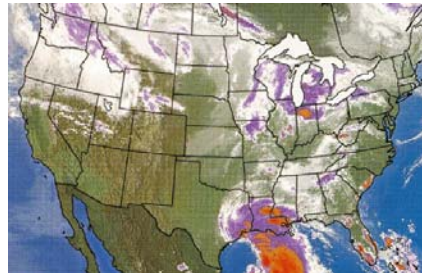
Geographic Map  
“precise outlines of the states”



## Fusion Images



Discovery PET/CT Images  
“abnormal activity **and** precise body’s anatomy”



USA Weather Map  
“intense weather **and** precise outlines of the states”

## PET/CT scanner:

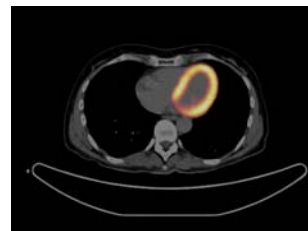
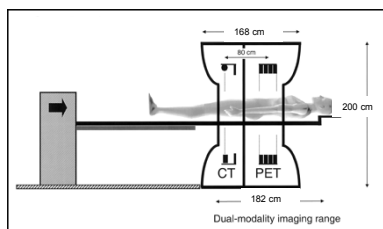
First “physicist’s” PET-CT was constructed by Townsend, Beyer, Kinahan et al in Pittsburgh 1994-

We (Rigshospitalet) got a prototype from GE in 2001

Today commercial devices exist from:

- GE
- Siemens
- Philips
- and a few others
- - with more than 5000 installations worldwide
  
- Since 2005, almost NO stand-alone PETs have been installed

## PET/CT (or SPECT/CT) scanner:



(Townsend et al 2004)

- combines two modalities in one gantry, common axis, common bed
- allows precise fusion of images
- provides structure + function in the same image
- can use CT for attenuation correction of PET /SPECT)

Anatomical localisation of tracer – Attenuation correction



# PET/CT: GE Discovery LS

Advance NXI + Lightspeed plus



Detector  
material  
BGO



\$2018

151

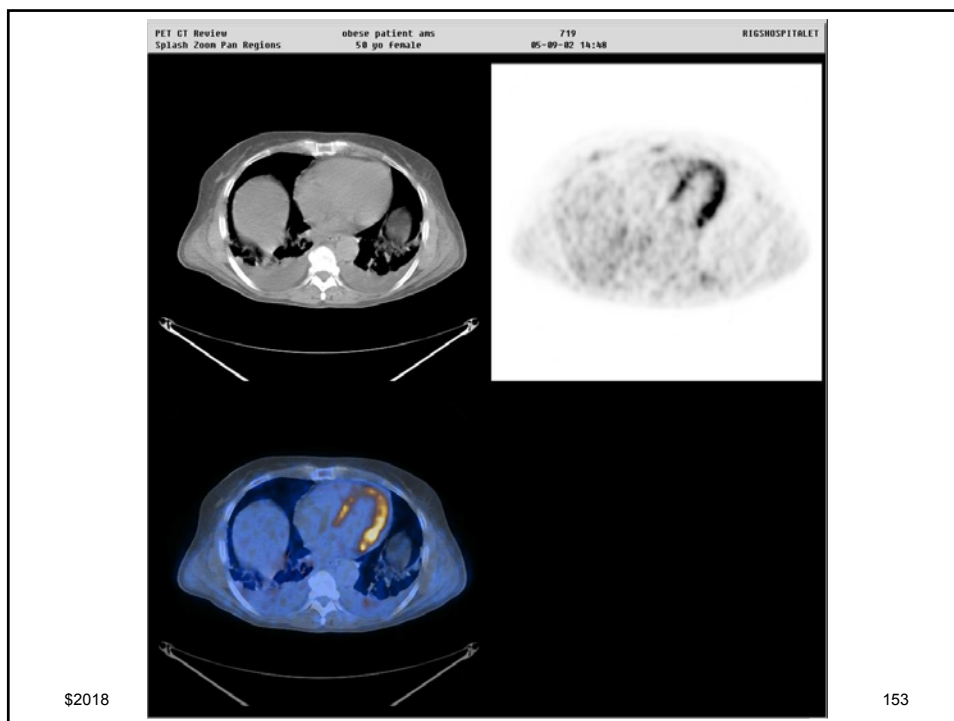


# Inside Discovery LS



\$2018

152





## PET/CT (images from around 2005)



Herlev  
Hillerød  
Vejle (2)  
Århus Skejby RT



**Philips Gemini** (KAS Herlev)

RH (5)  
Næstved (2)  
Århus PET (2)  
Århus NUK  
Herning  
Herlev (3)  
Glostrup



**Siemens Biograph** (RH)

\$2018



**GE Discovery** (Milano San Raffaele)

Odense (5)  
Ålborg (2)  
Køge (2)  
Århus Skejby  
Hvidovre  
Gentofte  
Bispebjerg (3)

154

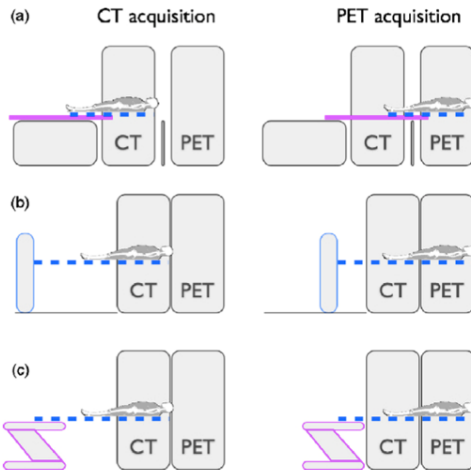
## PET/CT instrumentation: adding CT



- Important design criterion: keeping the patient position (height) stable



\$2018



155

## PET –CT alignment /registration



Not likely to change spontaneously.

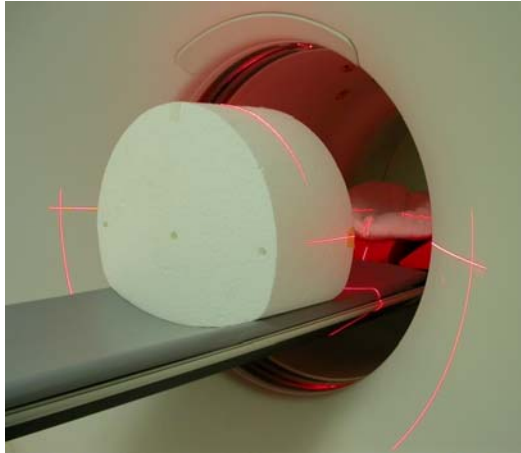
For **GE** and **Siemens**: Only opened by service. Must be measured after "invasive procedures"

**Philips Gemini** designed to scan in the separated position also.

\$2018

156

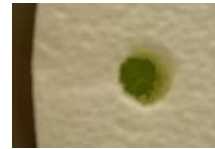
## GE PET – CT alignment



GE Discovery aligns CT with PET transmission using the built-in Ge-68 line sources.

No (other) activity is required  
The phantom contains 5 glass spheres

Newest GE-scanners use similar phantom with Ge-68 spheres



\$2018

157

## Siemens PET – CT alignment



Siemens Biographs have no transmission sources.

Instead 2 Ge-68 line sources mounted in a black box are used.

They are visible on both PET and CT, and an automated algorithm provides the correction

\$2018

158

## Philips PET – CT alignment

- Special service tool holding 6 Na-22 point sources
- Registration performed at 1 year interval



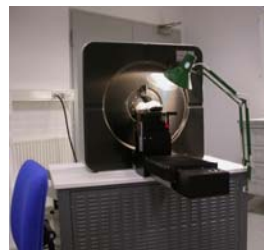
\$2018

159

## Small Animal PET-CT



CT resolution down to 15  $\mu$



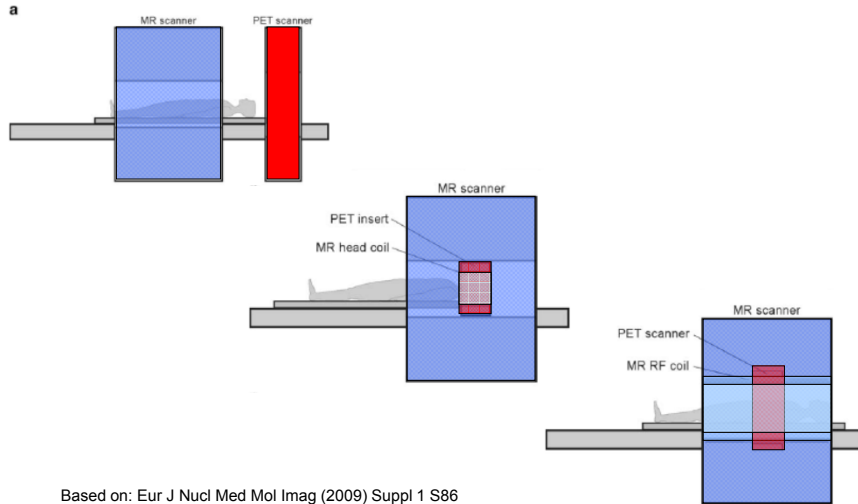
PET resolution < 2 mm



\$2018

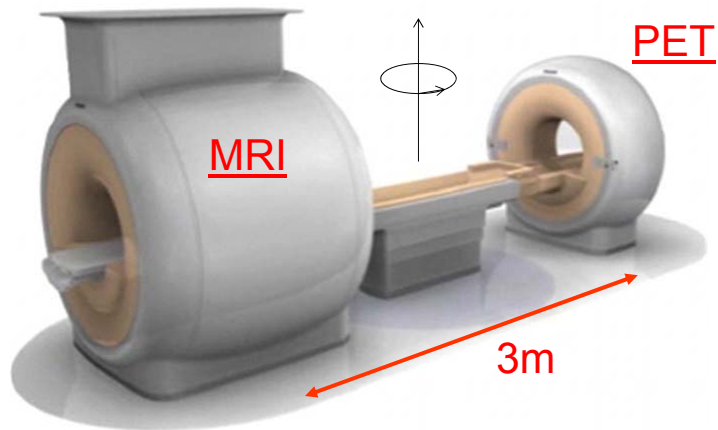
160

# Potential PET-MR configurations



Based on: Eur J Nucl Med Mol Imag (2009) Suppl 1 S86

# PET-MR: the "easy" solution



## PET-MR: the "easy" solution



Philips Medical, exhibition RSNA 2012

\$2018

163

## (real) PET-MR is now available



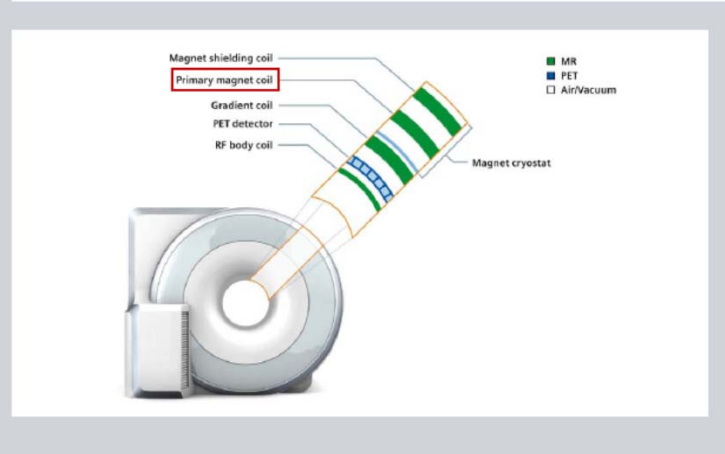
- Siemens made a prototype combination in 2007:
  - 3 T MR scanner with brain coil
  - PET "insert" between coil and magnet
  - Requires detector insensitive to magnetic field
- In 2011, Siemens made an integrated system (APD)
- In 2014, GE followed (SiPM – TOF possible)

\$2018

164

two is now one.  
**The first whole-body MR-friendly PET architecture**

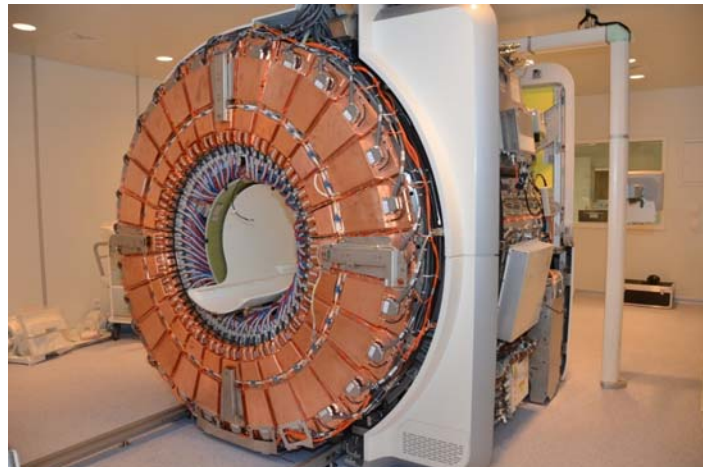
**SIEMENS**



\$2018

165

## PET/MR



All PET electronics is encapsulated in a Faraday cage to avoid RF-interference

\$2018

166



PET(/MR) service (PET module exchange)



\$2018

167



\$2018

Arrival: 29.November 2011

168



\$2018

Arrival: 29.November 2011

169

## Inauguration 14.December 2011



\$2018

170

## With PET/CT:

A CT scan is a  $\mu$ -map (expressed in HU)  
 A scaling for energy difference between CT and PET is required  
 Soft tissue and bone (and contrast) scale differently  
 $\Rightarrow$  (only) minor errors in quantitation of PET images



GE Discovery LS (2001)

## In PET/MR:

Attenuation correction is a challenge (and a current research topic)

MR images (in general) are NOT  $\mu$ -maps

Bone, Air, and Metal implants show almost same MR-signal:  $\sim 0$   
 - but they have very different influence on PET attenuation



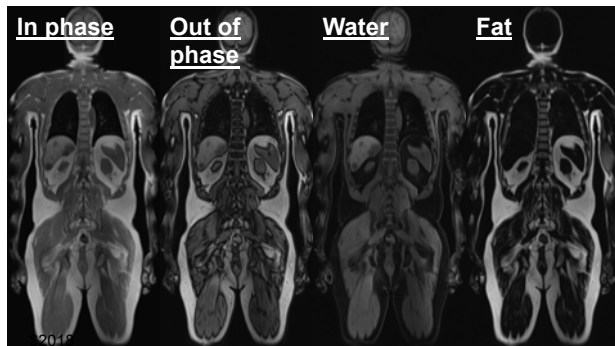
# MR-based attenuation correction



Dixon water/fat segmentation (DWFS)

\_Martinez-Möller et al., J Nucl Med (2009)

→ Water + Fat + Air + Lung. **No Bone.**

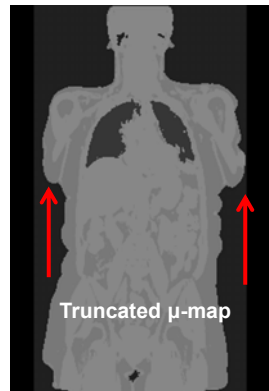
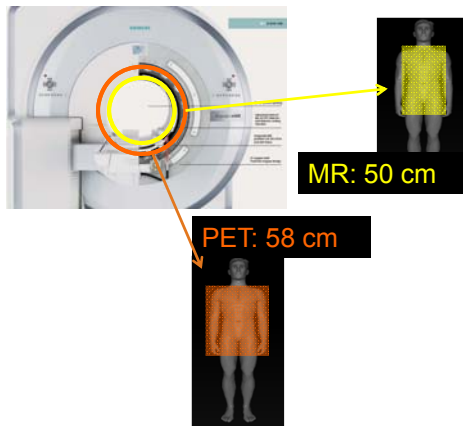


DWFS  $\mu$ -map



173

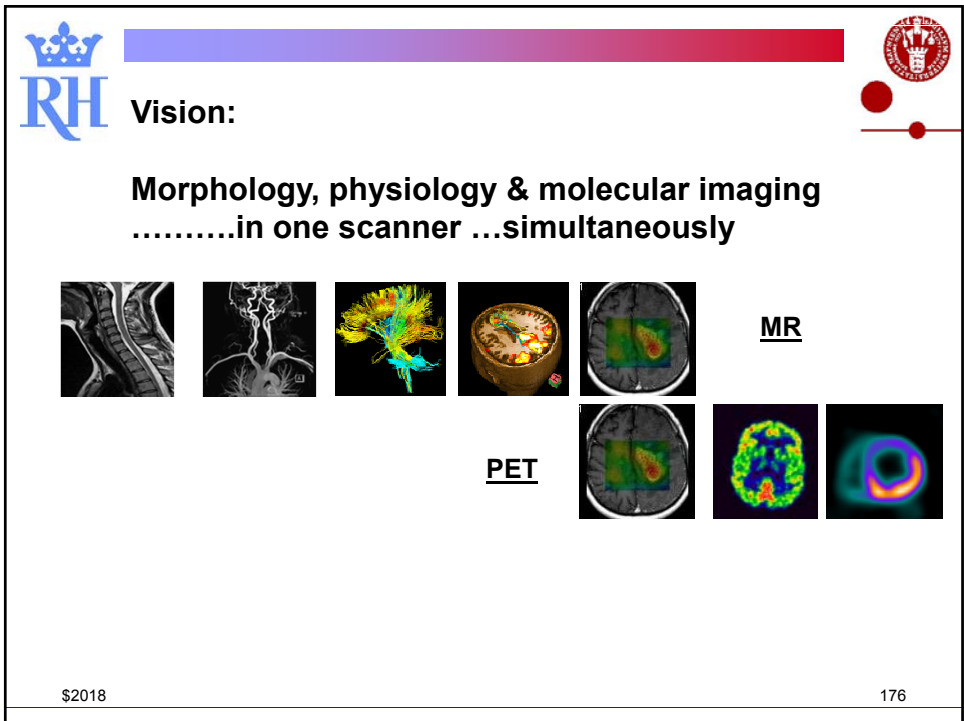
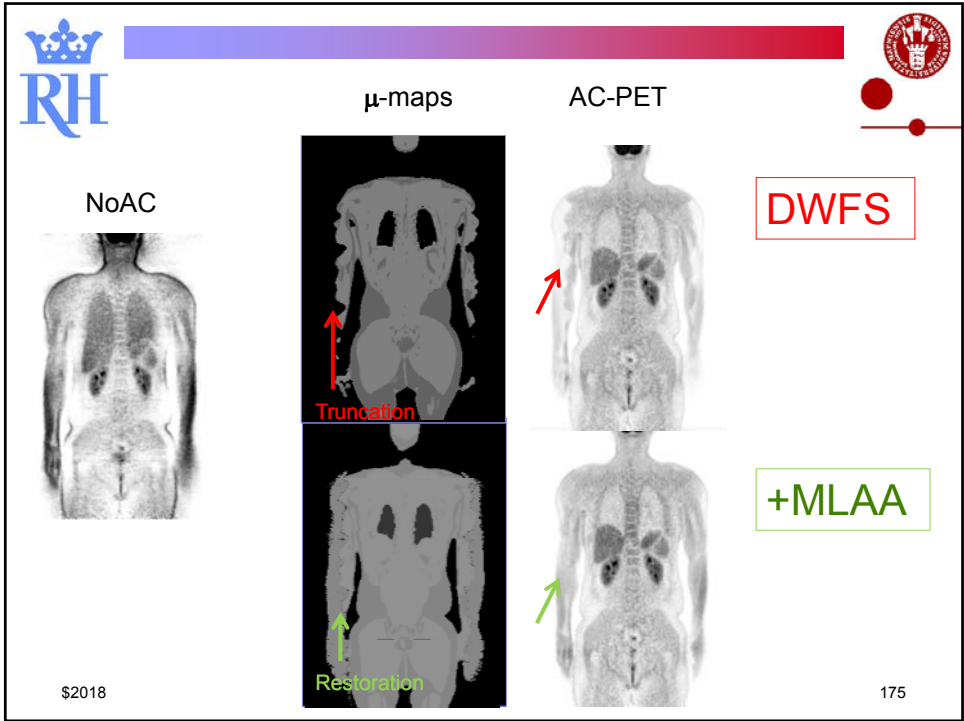
Truncation = Mismatch of transverse field-of-view  
 "Arms down" is standard position in PET/MR



S2018

[Keller et al. Magnet Reson Mater Phys \(2012\)](#)

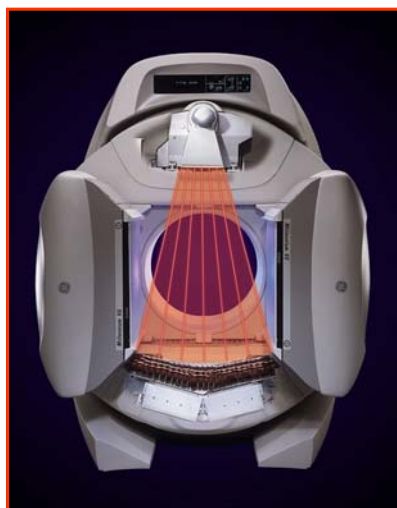
174



## SPECT/CT

- serves the same dual purpose of Anatomical localisation of tracer and Attenuation correction
- AC is not as simple or "exact" as in PET because we have only one photon
- With CT and iterative recon, quantitation is feasible

## SPECT/CT (GE Hawkeye)



X-Ray Tube is mounted on the same gantry as the gamma cameras

A 'CT scan' takes 15 s / cm

With 1 inch crystals, "PET" is possible



## SPECT/CT



Siemens



Symbia

\$2018

Philips

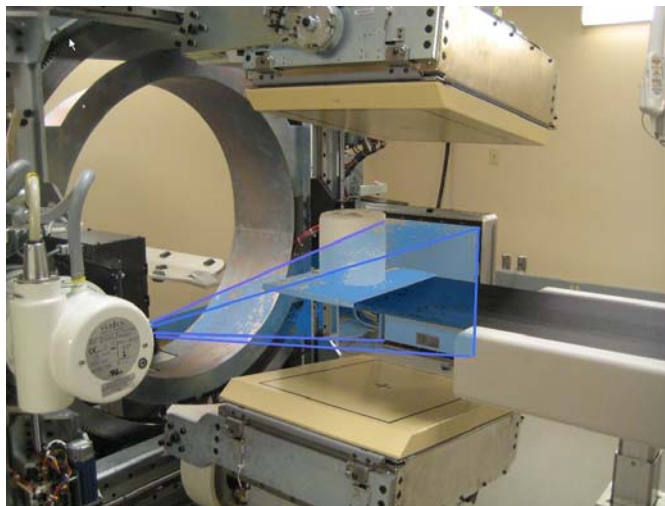


Precedence =

Skylight SPECT + Brilliance CT

179

## BrightView XCT SPECT/CT



\$2018

180

# Combinations...

PET-CT / SPECT-CT / PET-MRI / SPECT-MRI



\$2018

Exhibition EANM October 2012

181

# PET / SPECT / CT

for small animals



\$2018

182

## VECTOR: A Preclinical Imaging System for Simultaneous Submillimeter SPECT and PET

Marlies C. Goorden<sup>\*1</sup>, Frans van der Have<sup>\*1,2</sup>, Rob Kreuger<sup>1</sup>, Ruud M. Ramakers<sup>1,2</sup>, Brendan Vastenhouw<sup>1,2</sup>, J. Peter H. Burbach<sup>3</sup>, Jan Booij<sup>4</sup>, Carla F.M. Molthoff<sup>5</sup>, and Freck J. Beekman<sup>1,2</sup>

J Nucl Med 2013; 54:306–312  
DOI: 10.2967/jnumed.112.109538

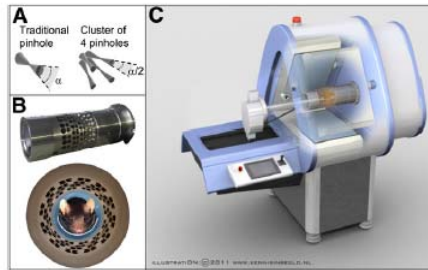


**FIGURE 1.** Integration of clustered-pinhole collimator into existing SPECT/CT platform. (A) Traditional pinhole with opening angle  $\alpha$  and cluster of 4 pinholes with approximately same field of view and opening angle  $\alpha/2$ . (B) Clustered-pinhole collimator optimized for imaging SPECT and PET tracers, into which mouse is placed. (C) Collimator mounted in SPECT/CT system.

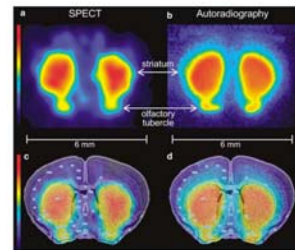


**Figure 2.** High resolution in vivo imaging of striatal DAT Dfdr compared with DAT autoradiography (right).

\$2018

183

## G-SPECT

• Game-Changing SPECT



\$2018

184



## Spectrum Dynamics D-SPECT



CZT  
= CdZnTe

\$2018

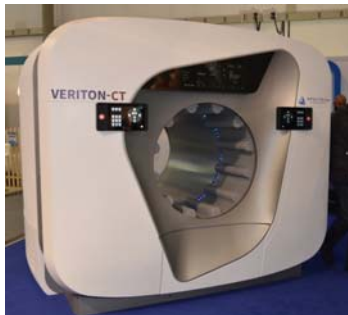
185



## Spectrum Dynamics Veriton-CT



CZT = CdZnTe



\$2018

186



# PET / SPECT / CT



AnyScan

Mediso  
Budapest

Exhibition at  
EANM 2008  
Still marketed

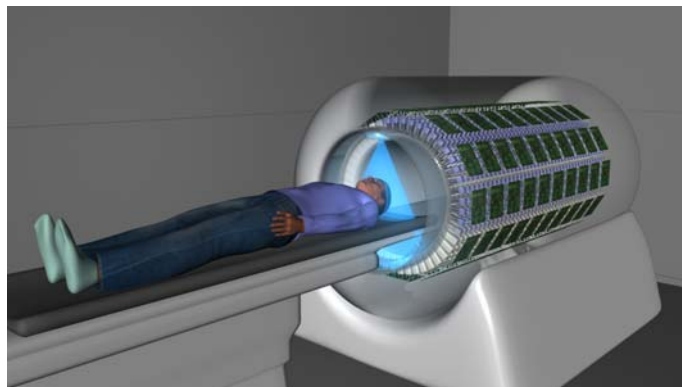


\$2018

187



# EXPLORER



**UC DAVIS**  
UNIVERSITY OF CALIFORNIA

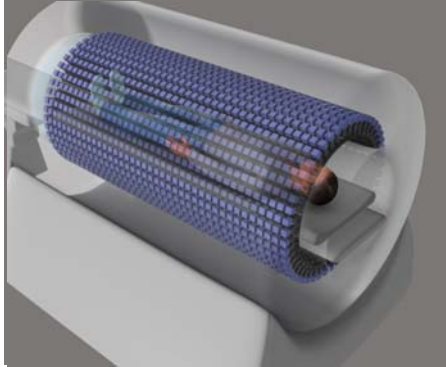


**Penn**  
UNIVERSITY OF PENNSYLVANIA

\$2018

188

## Maximizing Sensitivity by Total-Body PET



**~40-fold** increase  
for adult total-body imaging

**~20-fold** increase  
for pediatric total-body imaging

**~4-fold** increase  
for single organ imaging

\$2018

189

## Applications

### Systemic disease and therapies:

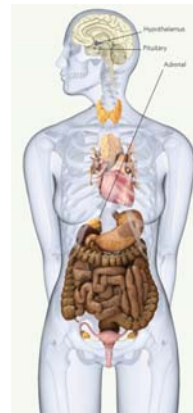
- Cancer: Ultra-staging and micrometastasis
- Inflammation
- Infection
- Cellular therapy and trafficking
- Mind-body interactions

### Total body pharmacokinetics

- Drug development
- Toxicology
- Biomarker discovery

### Low dose opens up new populations:

- Expanded use in pediatrics
- Use in chronic disease
- Studies of normal biology



\$2018

190

# Completed EXPLORER Scanner

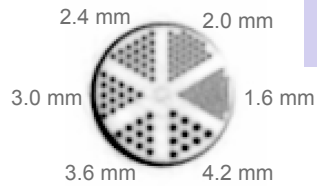
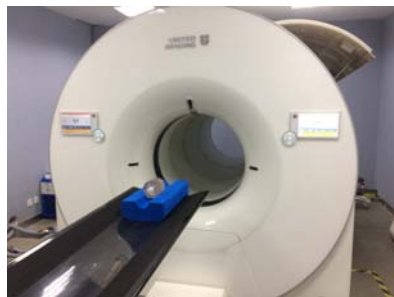
**System:**  
 Ring diameter: 78.6 cm  
 Transaxial FOV: 68.6 cm  
 Axial FOV: 194.8 cm  
  
 # of crystals: 564,480  
 # crystal blocks: 13,440  
 # of SiPMs: 53,760  
  
 80 detector row CT



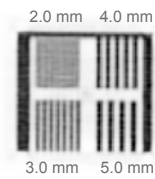
\$2018

191

# Preliminary Resolution Tests



**mini Derenzo:**  
 8 billion prompts  
 transaxial slice



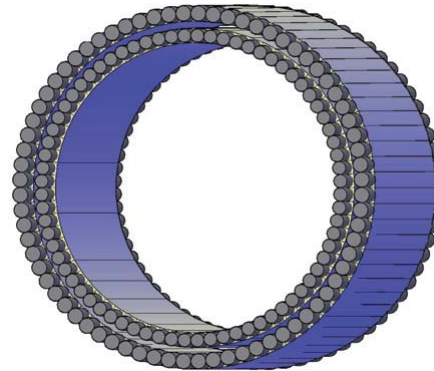
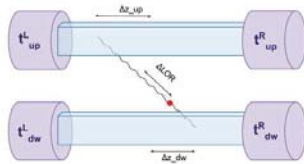
**axial bar:**  
 12 billion prompts  
 sagittal slice

\$2018

192

# J-PET

Longitudinal plast-scintillators



P Moskal *et al*  
 Phys. Med. Biol. **61** (2016) 2025

## Advances in Dynamic Radioactive Scanning

Compiled and Edited by

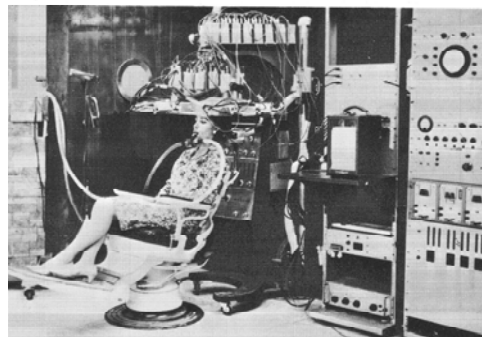
YEN WANG, M.D., D.Sc. (MED.)

Associate Professor of Radiology  
 University of Pittsburgh  
 and  
 Chairman, Department of Radiology  
 Homestead Hospital  
 Pittsburgh, Pennsylvania



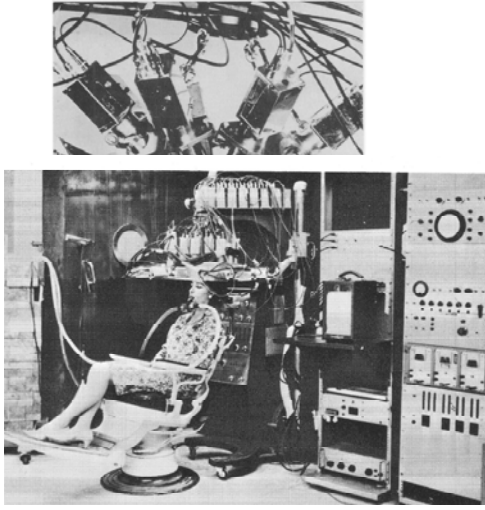
CHARLES C THOMAS • PUBLISHER  
 Springfield • Illinois • U.S.A.

## 1968 PET



1966

2015



1966 Brookhaven 1966 – moved to MNI 1968

Development of the Helmet-Chin PET Prototype

Hidetaka Yoshida, Eiji Yoshida, Fumihiko Nishikubo, Hidetaka Wakana, Masataka Niwa, Abdellatif M. Akhmet, Akram Mohamed, Shinsuke Tazawa, Yasuyuki Kaneko, Teruya Sakata, Yasuhisa Fujihayashi, and Tsugu Yasuura, Member, IEEE

Chiba, Japan [Poster M3CP-97 at MIC2015]

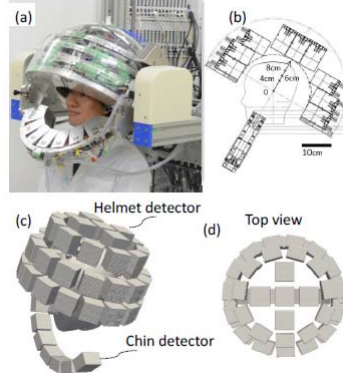
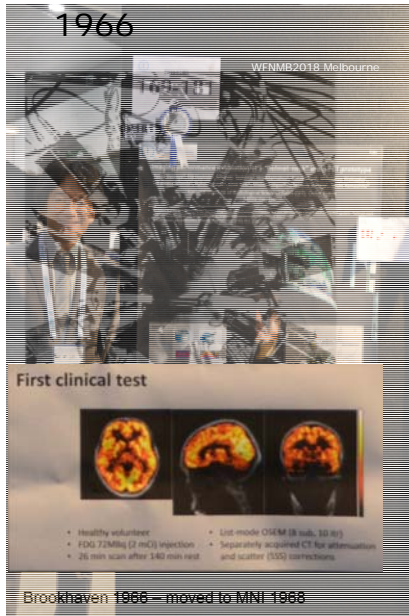


Fig. 1. Photograph of the first prototype of the helmet-chin PET (a), design sketch (b), and geometry of the crystals (c), (d).

1966

2015



2018 Brookhaven 1966 – moved to MNI 1968

Development of the Helmet-Chin PET Prototype

Hidetaka Yoshida, Eiji Yoshida, Fumihiko Nishikubo, Hidetaka Wakana, Masataka Niwa, Abdellatif M. Akhmet, Akram Mohamed, Shinsuke Tazawa, Yasuyuki Kaneko, Teruya Sakata, Yasuhisa Fujihayashi, and Tsugu Yasuura, Member, IEEE

Chiba, Japan [Poster M3CP-97 at MIC2015]

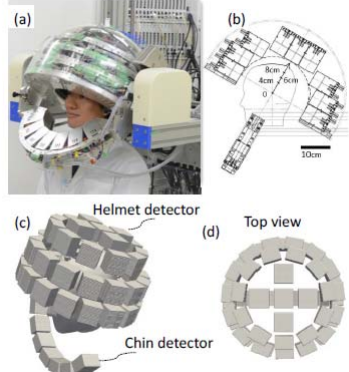


Fig. 1. Photograph of the first prototype of the helmet-chin PET (a), design sketch (b), and geometry of the crystals (c), (d).

### Could this become a "trend" ?

**IF** a cure for, e.g. Alzheimer's disease is found

**AND**

**IF** we have a PET-tracer that can tell if that cure works for YOU

**AND**

**IF** this device can be manufactured for  $\frac{1}{4}$  of the price of WB PET/CT

**THEN** it is likely to.



Time to  
press...

